Electronic Supplementary Information (ESI)

For

Aggregation-induced emission active seminaphthofluoresceins: A new class of xanthene luminogens for bioimaging

*Laura McKay,[a] Issan Zhang,[b] Imogen Suh,[a] D. Scott Bohle,[a] Ashok Kakkar,[*a] and Dusica Maysinger [*b]*

[a.] Department of Chemistry, McGill University, 801 Sherbrooke St. West, Montreal, Quebec, Canada
[b.] Department of Pharmacology and Therapeutics, McGill University, 3655 Promenade Sir-William-Osler, Montreal, Quebec, Canada

Table of Contents

1. Synthesis and Characterization

1.1 Synthetic Schemes and Methods

*Synthesis of TPRP-SNAFL (**1**)*

A two neck round bottom flask containing 0.18 g. (0.42 mmol) of 5-carboxy-seminaphthofluorescein was purged with nitrogen before the addition of 15 mL of HPLC grade acetone. Solid potassium carbonate (0.41 g) was added, followed by the slow addition of propargyl bromide solution (80% in toluene) by syringe (0.40 mL, 4.3 mmol). The reaction was heated to 60°C and allowed to proceed under nitrogen flow for 85 h, during which time the hue of the mixture transitioned from a pale brown to deep purple. The solvent was removed under reduced pressure and the resulting purple solid was transferred to a separatory funnel with 200 mL ethyl acetate and 50 mL of deionized water. The organic layer was separated and washed with 50 mL portions of water and saturated brine solution. The solution was dried with magnesium sulfate before the solvent was removed to yield the crude material as a foaming red-purple solid. The residue was loaded onto a moderate length column and eluted with 7.5% methanol in dichloromethane to yield 0.081 g (0.41mmol, 36 %) of **1** as a reflective red powder.

*Synthesis of 2-(2,4-dihydroxybenzoyl)benzoic acid (**I-1**)*

To a one neck 100 mL round bottom flask equipped with a condenser was added 45 mL of deionized water. In portions, 45 g. of sodium hydroxide pellets (50% by mass) were added to solution. After a cooling period of 45 minutes 9.55 g of purified commercial fluorescein (28.7 mmol) was added to the flask. The deep purple solution was heated to 90 °C for a period of 20 h, after which the medium brown mixture was cooled to room temperature and poured into 250 mL of chilled deionized water. The flask was placed in a secondary ice/brine bath and set to stir vigorously before initiating dropwise addition of 12 M HCl. The addition was continued over a period of 2 h and slowed as the solution reached acidity. At a pH of ~1 a beige solid precipitated rapidly, at which point the stirring rate was increased and addition was stopped. The solids were allowed to stir for 1 h and settle overnight at room temperature. The crude product was collected on a medium grain frit and dried for 24 h. on house vacuum. After an additional 1 h under high vacuum the solid was taken up in 100 mL of diethyl ether and washed with 25 mL portions of water and brine. The ethereal solution was dried with magnesium sulphate and the solvent removed under reduced pressure to yield 2.84 g. (11.1 mmol, 38%) of the benzophenone as a light-yellow solid.

*Synthesis of Seminaphthofluorescein-C (**I-2**)*

A two neck 50 mL round bottom flask under nitrogen was charged with 1.02 g (4.0 mmol) of **I-1** and 0.63 g (4.0 mmol) of 1,6-naphthalene diol. Through a rubber septum 5 mL of methane sulfonic acid and 5 mL of trifluoroacetic acid were added and the reaction was allowed to proceed at room temperature, shielded from light, for 22 hours. The teal solution was then opened to air and poured into 250 mL of chilled deionized water with immediate precipitation of the crude product. The deep purple solid was collected on a fine grain frit, washed with 3x20 mL portions of water on the frit, and allowed to dry under house vacuum for 24 h. A solution of the crude product in 125 mL of 2 M NaOH was prepared in a 500 mL conical flask. Dropwise addition of 130 mL of 2 M HCl with vigorous stirring resulted in precipitation of a fine purple solid which was collected and dried thoroughly under vacuum. The collected material was dissolved in 50 mL of anhydrous ethanol and added dropwise to 250 mL of deionized water with vigorous stirring. The resulting precipitate was allowed to settle at room temperature before collection on a fine grain frit. The title compound, a shiny deep purple solid reflecting green, was obtained in 86% yield (1.31 g, 3.4 mmol).

*Synthesis of DPRP-SNAFL (**2**)*

A two neck round bottom flask containing 0.70 g. (1.8 mmol) of seminaphthofluorescein **I-2** was purged with nitrogen before the addition of 30 mL of HPLC grade acetone. Solid potassium carbonate (1.80 g, 13.0 mmol) was added, followed by the slow addition

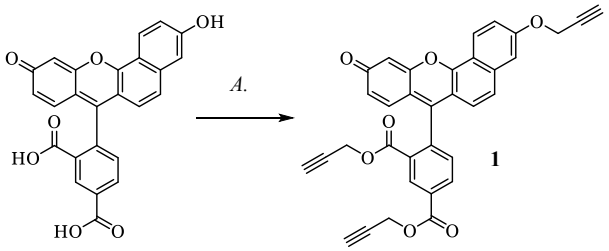

Scheme S.1 Synthesis of TPRP-SNAFL **(1)** from 5-carboxy-seminaphthofluorescein. A) Propargyl bromide, K_2CO_3, acetone, 60 °C, 85 h.

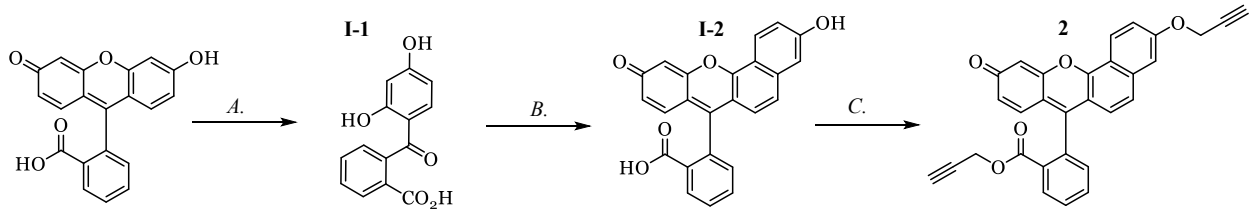

Scheme S.2 Synthesis of DPRP-SNAFL **(2)** from seminaphthofluorescein. A) NaOH (50% w/w, aq.), 90 ◦C, 20 h ; B) 1,6-naphthalene diol, $MeSO_3H$/TFA, RT, 22 h ; C) Propargyl bromide, K_2CO_3, acetone, 60 ◦C, 48 h.

of propargyl bromide solution (80% in toluene) by syringe (0.84 mL, 9.1 mmol). The reaction was heated to 60°C and allowed to proceed under nitrogen flow for 45 h, during which time the hue of the mixture transitioned from a pale brown to deep purple. The solvent was removed under reduced pressure and the resulting purple solid was transferred to a separatory funnel with 200 mL ethyl acetate and 50 mL of deionized water. The organic layer was separated and washed with 50 mL portions of water and saturated brine solution. The solution was dried with magnesium sulfate before the solvent was removed to yield the crude material as a foaming red-purple solid. The residue was loaded onto a moderate length column and eluted with 5% methanol in dichloromethane to yield 0.40 g (0.87mmol, 48 %) of **2** as a reflective red powder.

1.2 NMR and HRMS Data

*TPRP-SNAFL (**1**)*

^{1}H NMR (500 MHz, $(CD_3)_2CO$) δ 8.88 (d, *J* = 1.7 Hz, 1H), 8.62 (d, *J* = 9.2 Hz, 1H), 8.52 (dt, *J* = 7.9, 1.6 Hz, 1H), 7.79 (dd, *J* = 8.0, 1.5 Hz, 1H), 7.61 (d, *J* = 8.9 Hz, 1H), 7.53 (d, *J* = 2.5 Hz, 1H), 7.45 (dd, *J* = 9.2, 2.5 Hz, 1H), 6.98 (dt, *J* = 9.6, 1.4 Hz, 2H), 6.51 – 6.42 (m, 2H), 5.13 (d, *J* = 2.5 Hz, 2H), 5.00 (d, *J* = 2.4 Hz, 2H), 4.76 – 4.63 (m, 2H), 3.22 (t, *J* = 2.5 Hz, 1H), 3.19 (t, *J* = 2.4 Hz, 1H), 2.87 (t, *J* = 2.5 Hz, 1H).

^{13}C NMR (126 MHz,) $CD_3)_2CO$ δ 184.97, 164.91, 164.49, 159.70, 159.42, 150.41, 149.14, 140.69, 138.40, 134.80, 132.84, 132.74, 132.15, 131.51, 130.60, 125.23, 124.61, 124.43, 120.72, 119.82, 119.04, 115.75, 109.53, 106.07, 79.16, 78.59, 77.75, 77.71, 77.18, 76.98, 56.77, 53.81, 53.70.

HRMS (ESI$^+$) Anal. Calc. for $C_{34}H_{21}O_7$ (M+H$^+$) 541.1282 Found: 541.1290

*2-(2,4-dihydroxybenzoyl)benzoic acid (**I-1**)*

^{1}H NMR (500 MHz, $(CD_3)_2SO$) δ 13.16 (s, 1H), 12.22 (s, 1H), 10.69 (s, 1H), 7.98 (dd, *J* = 7.8, 1.3 Hz, 1H), 7.71 (td, *J* = 7.5, 1.3 Hz, 1H), 7.63 (td, *J* = 7.6, 1.3 Hz, 1H), 7.41 (dd, *J* = 7.5, 1.3 Hz, 1H), 6.91 (d, *J* = 8.8 Hz, 1H), 6.31 (d, *J* = 2.3 Hz, 1H), 6.27 (dd, *J* = 8.8, 2.3 Hz, 1H).

^{13}C NMR (126 MHz,) $CD_3)_2SO$ δ 200.58, 166.83, 165.08, 164.49, 140.05, 134.80, 132.32, 130.05, 129.77, 129.58, 127.49, 113.35, 108.39, 102.62.

HRMS (ESI$^+$) Anal. Calculated for $C_{14}H_9O_5$ (M+H$^+$) 257.0457 Found: 257.0456

*Seminaphthofluorescein-C (**I-2**)*

^{1}H NMR (500 MHz, $(CD_3)_2CO$) δ 9.11 (s, 1H), 9.03 (s, 1H), 8.48 (d, *J* = 9.0 Hz, 1H), 8.04 (dd, *J* = 7.5, 1.3 Hz, 1H), 7.83-7.73 (m, 2H), 7.40 (d, *J* = 8.8 Hz, 1H), 7.35 – 7.31 (m, 2H), 7.25 (d, *J* = 2.4 Hz, 1H), 7.03 (d, *J* = 2.4 Hz, 1H), 6.78 – 6.70 (m, 3H).

^{13}C NMR (126 MHz,) $CD_3)_2CO$ δ 169.49, 160.12, 157.93, 154.24, 152.69, 147.75, 137.06, 135.92, 130.57, 129.95, 127.41, 125.18, 124.93, 124.77, 124.43, 122.78, 119.38, 118.65, 113.57, 111.16, 110.90, 110.16, 103.34, 83.72.

HRMS (ESI$^+$) Anal. Calculated for $C_{24}H_{15}O_5$ (M+H$^+$) 383.0914 Found: 383.0920

*DPRP-SNAFL (**2**)*

^{1}H NMR (500 MHz, $(CD_3)_2CO$) δ 8.63 (d, *J* = 9.2 Hz, 1H), 8.32 (dd, *J* = 7.9, 1.3 Hz, 1H), 7.95 (td, *J* = 7.6, 1.4 Hz, 1H), 7.85 (td, *J* = 7.7, 1.3 Hz, 1H), 7.64 – 7.56 (m, 2H), 7.52 (d, *J* = 2.5 Hz, 1H), 7.44 (dd, *J* = 9.2, 2.6 Hz, 1H), 6.99 – 6.85 (m, 2H), 6.51 – 6.42 (m, 2H), 5.01 (d, *J* = 2.4 Hz, 2H), 4.69 – 4.57 (m, 2H), 3.18 (t, *J* = 2.4 Hz, 1H), 2.82 (t, *J* = 2.5 Hz, 1H).

^{13}C NMR (126 MHz,) $CD_3)_2CO$ δ 184.94, 165.16, 159.49, 150.28, 138.19, 135.72, 134.23, 131.93, 131.73, 131.18, 130.77, 130.63, 125.08, 124.41, 124.37, 120.50, 119.72, 118.92, 116.04, 109.36, 105.78, 79.18, 77.69, 77.67, 76.64, 56.65, 53.19.

HRMS (ESI$^+$) $C_{30}H_{19}O_5$ (M+H$^+$) 459.12270 Found: 459.12078

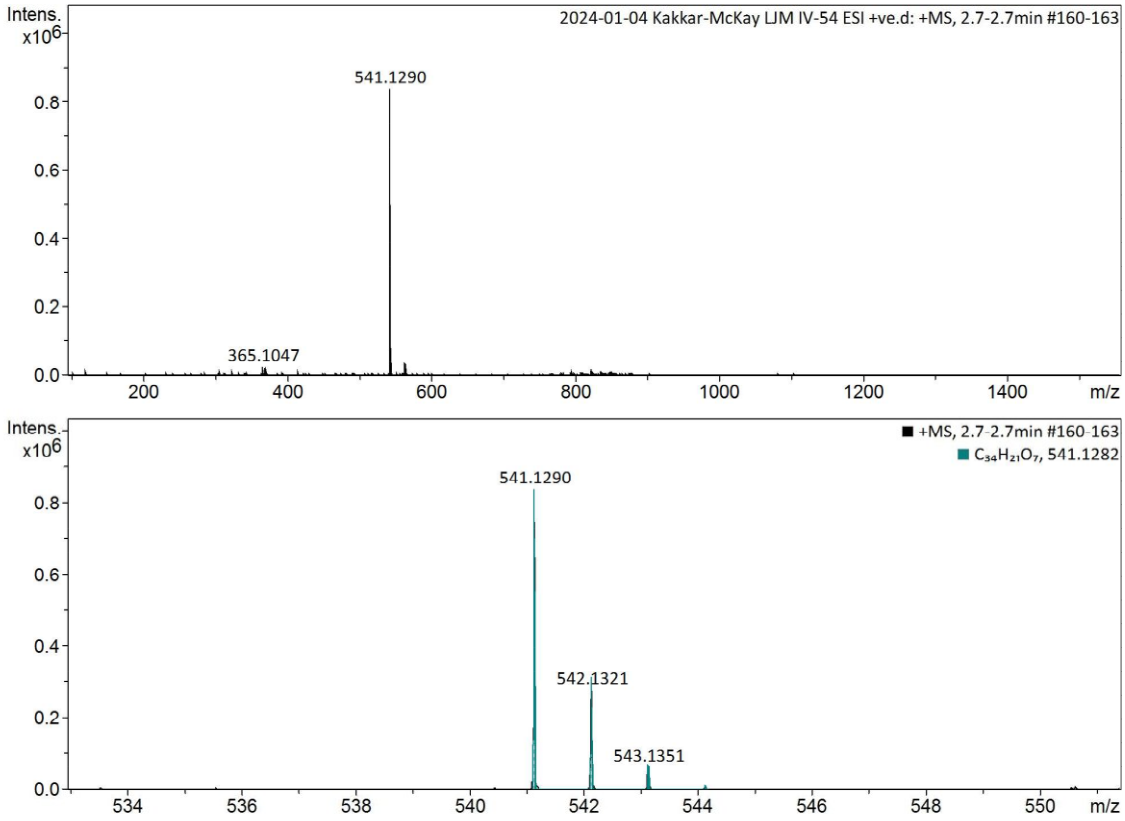

Figure S.1 *High resolution mass spectrum of TPRP-SNAFL* ***(1)***

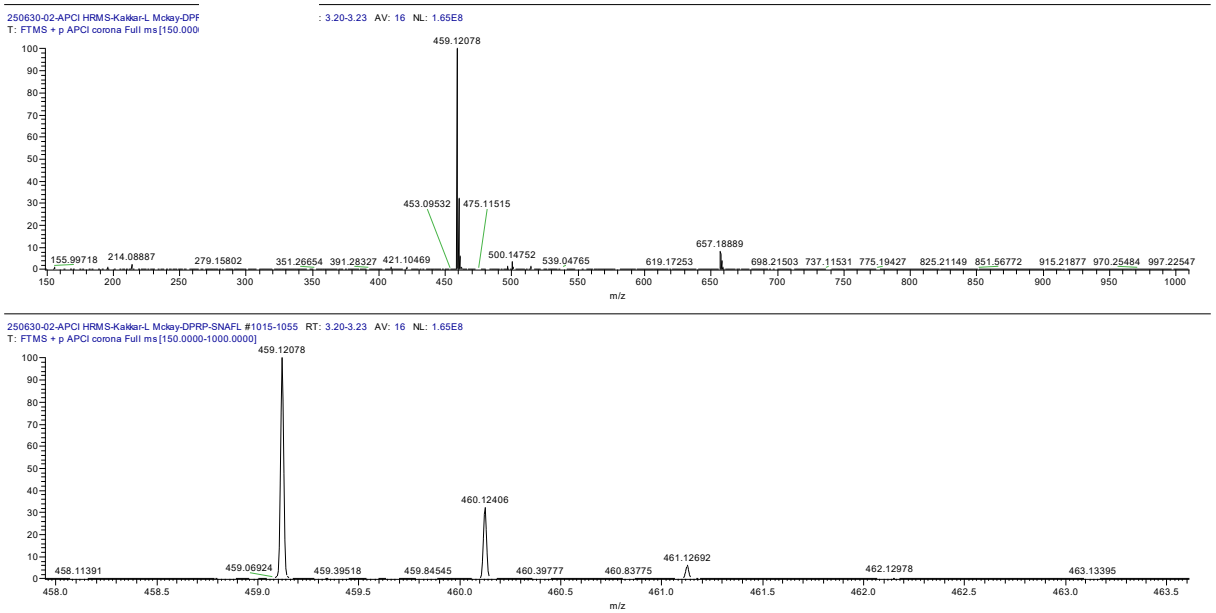

250630-02-APCI HRMS-Kakkar-L Mckay-DPRP-SNAFL#1040-1055 RT: 3.20-3.23 AV: 16
T: FTMS + p APCI corona Full ms [150.0000-1000.0000]
m/z= 459.09417-459.13571

Figure S.2 *High resolution mass spectrum of DPRP-SNAFL* ***(2)***

1.3 NMR Spectra

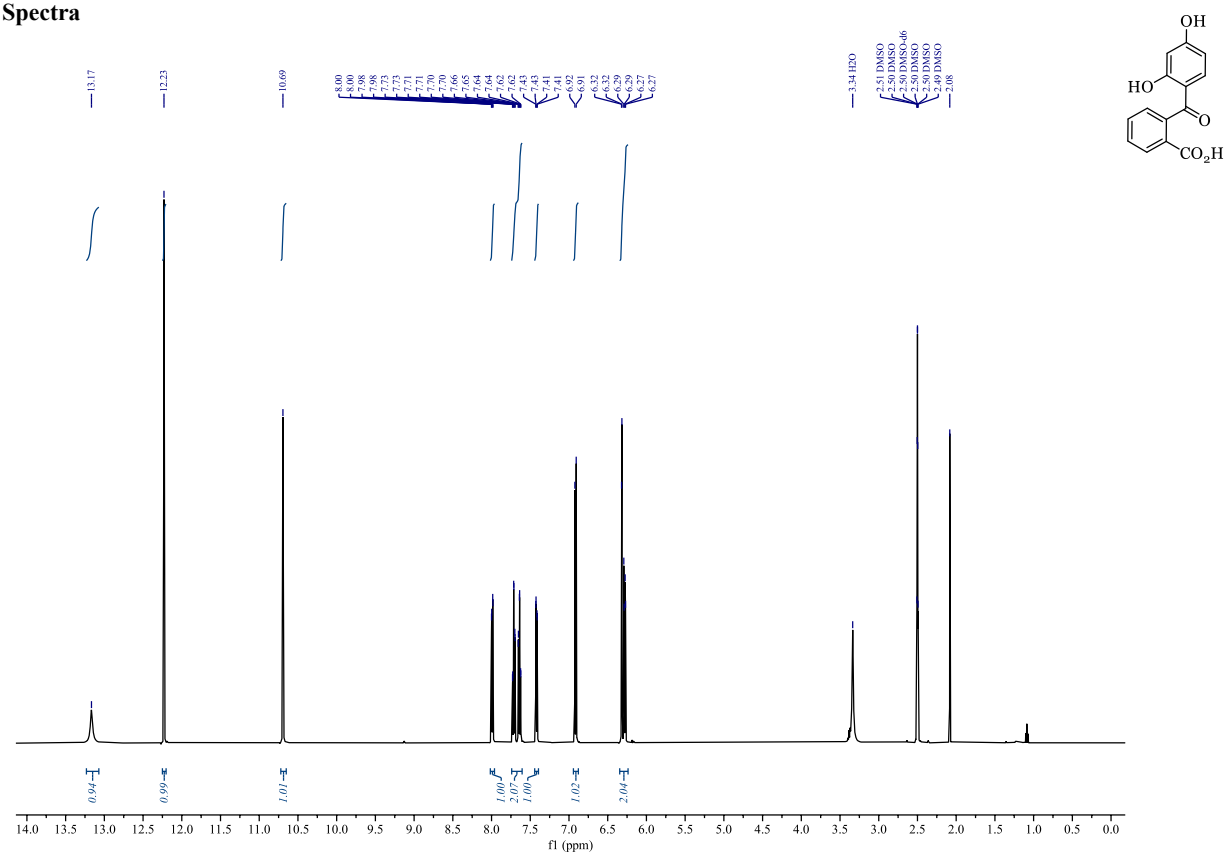

Figure S.3 *^{1}H NMR (500 MHz, $(CD_3)_2SO$) spectrum of 2-(2,4-dihydroxybenzoyl)benzoic acid (**I-1**)*

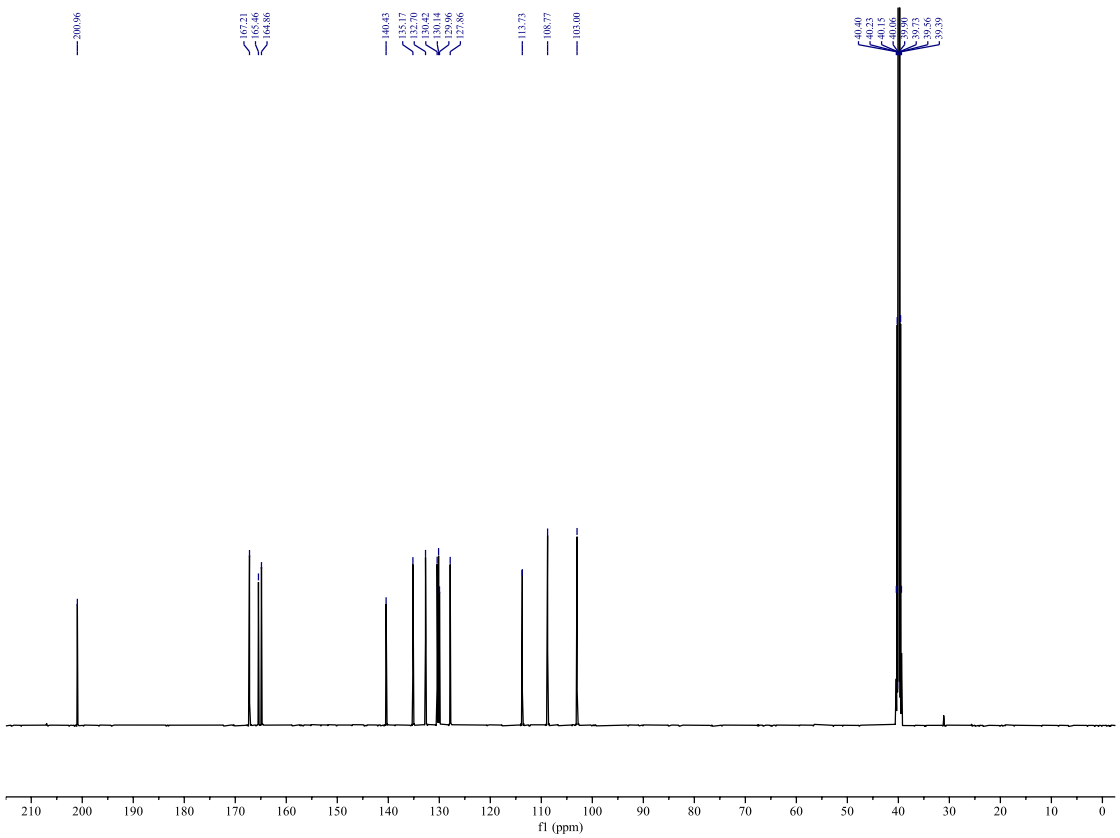

Figure S.4 *^{13}C NMR (126 MHz, $(CD_3)_2SO$) spectrum of 2-(2,4-dihydroxybenzoyl)benzoic acid (**I-1**)*

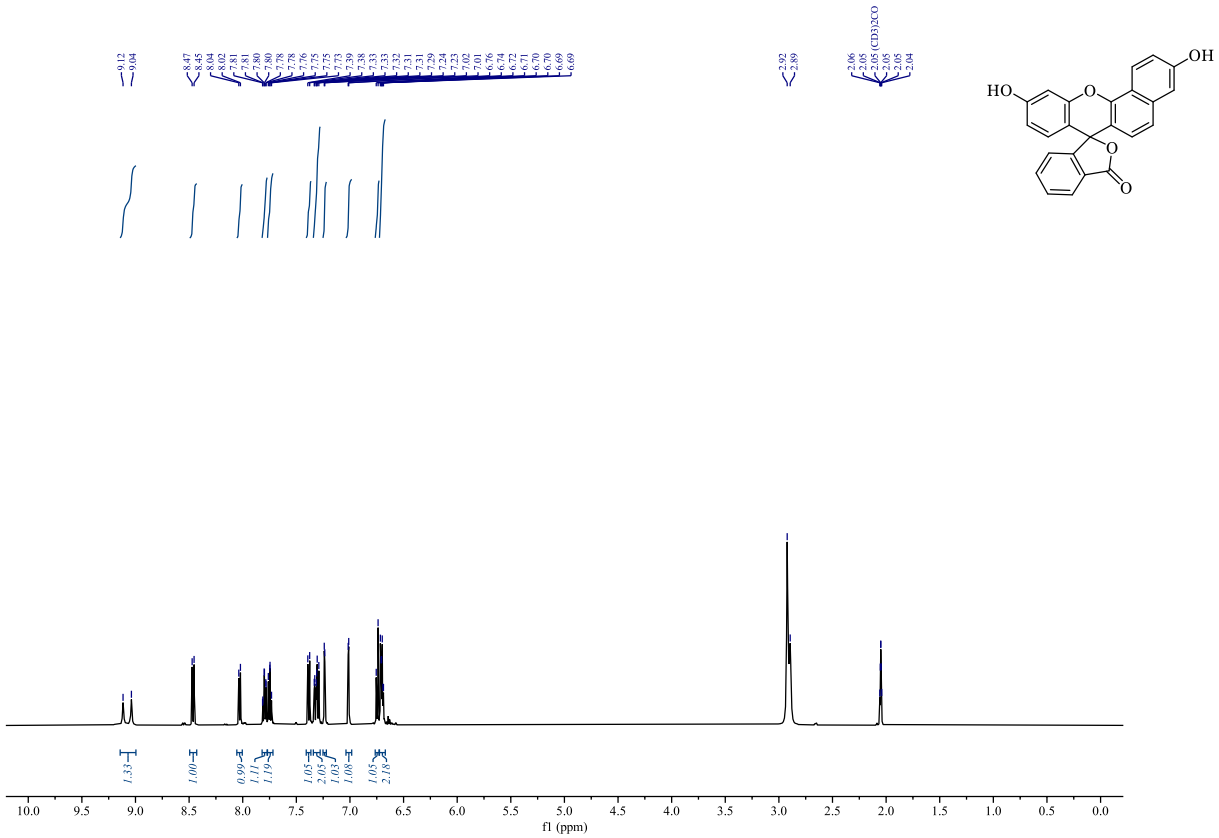

Figure S.5 *^{1}H NMR (500 MHz, $(CD_3)_2CO$) spectrum of seminaphthofluorescein (**I-2**, lactone form)*

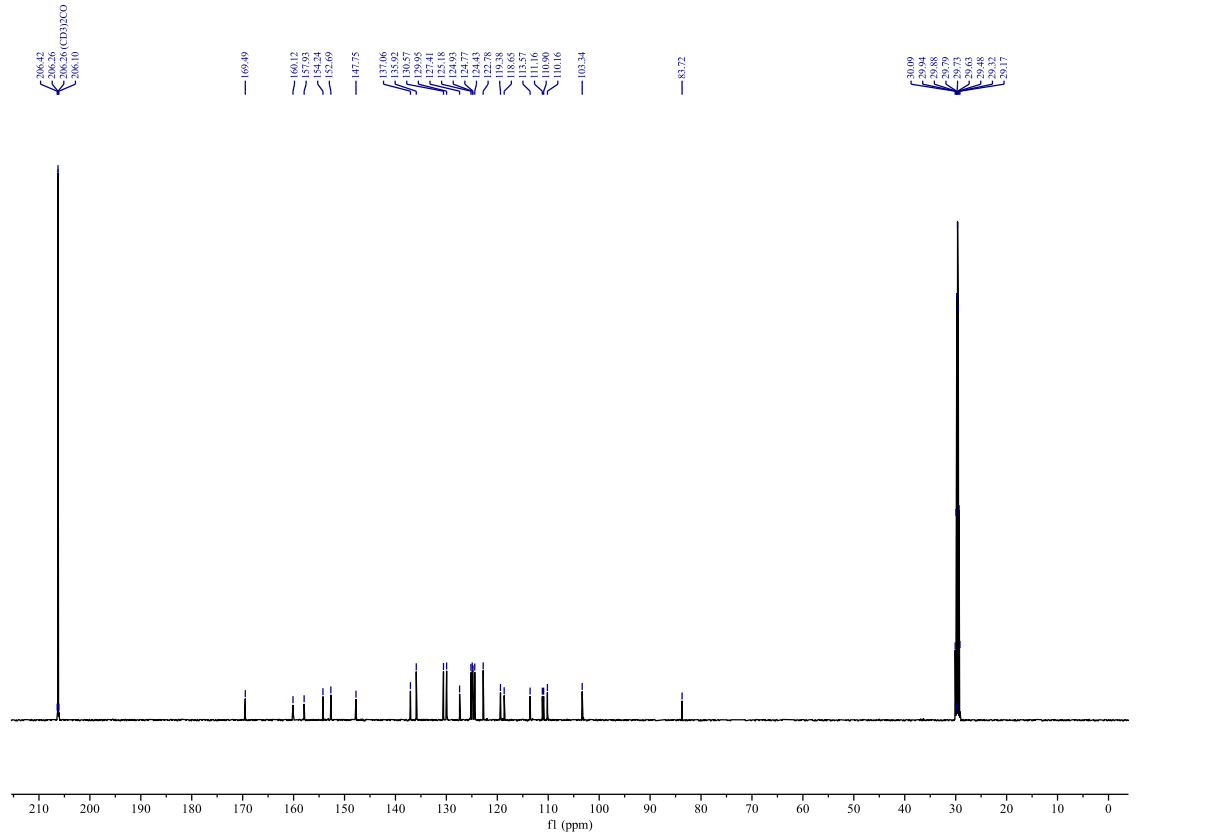

Figure S.6 *^{13}C NMR (126 MHz, $(CD_3)_2CO$) spectrum of seminaphthofluorescein (**I-2,** lactone form)*

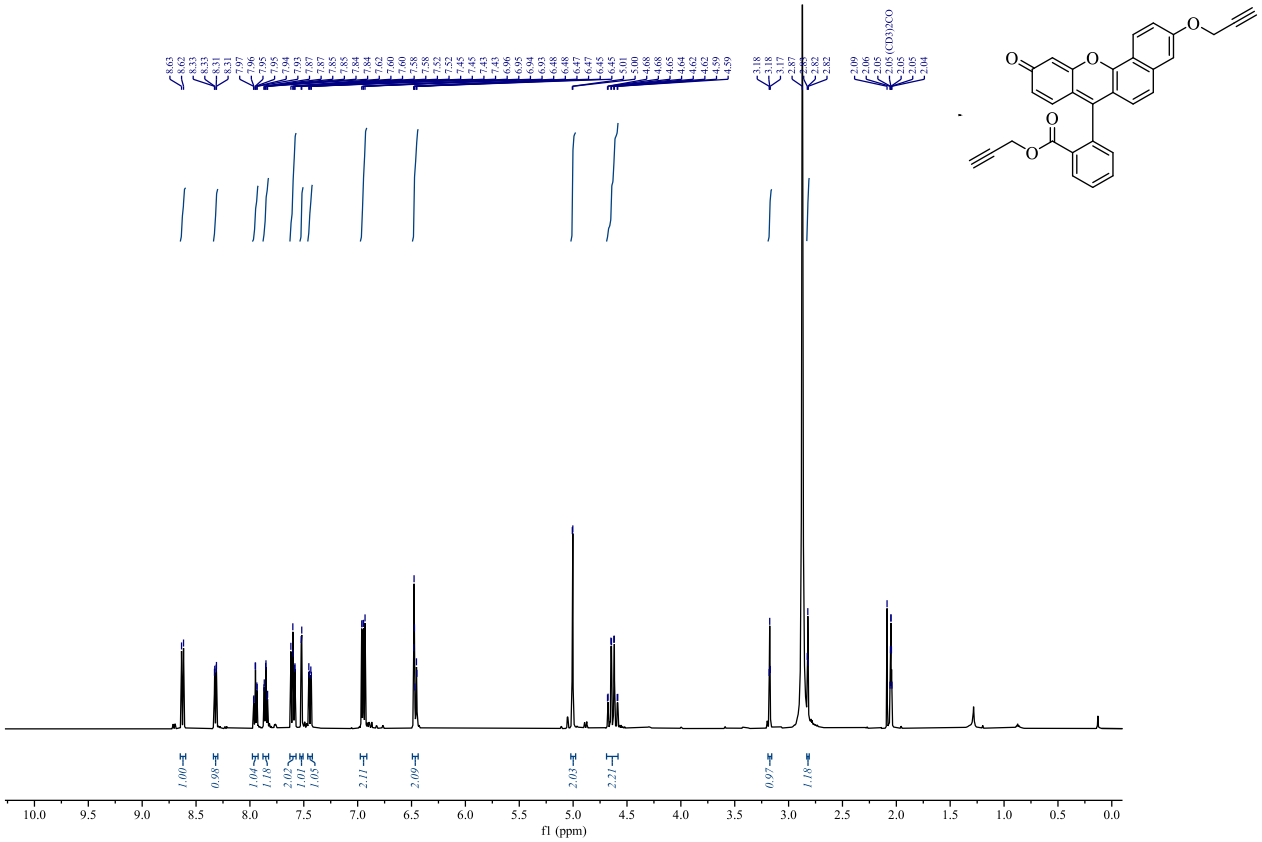

Figure S.7 *^{1}H NMR (500 MHz, $(CD_3)_2CO$) spectrum of DPRP-SNAFL (**2**)*

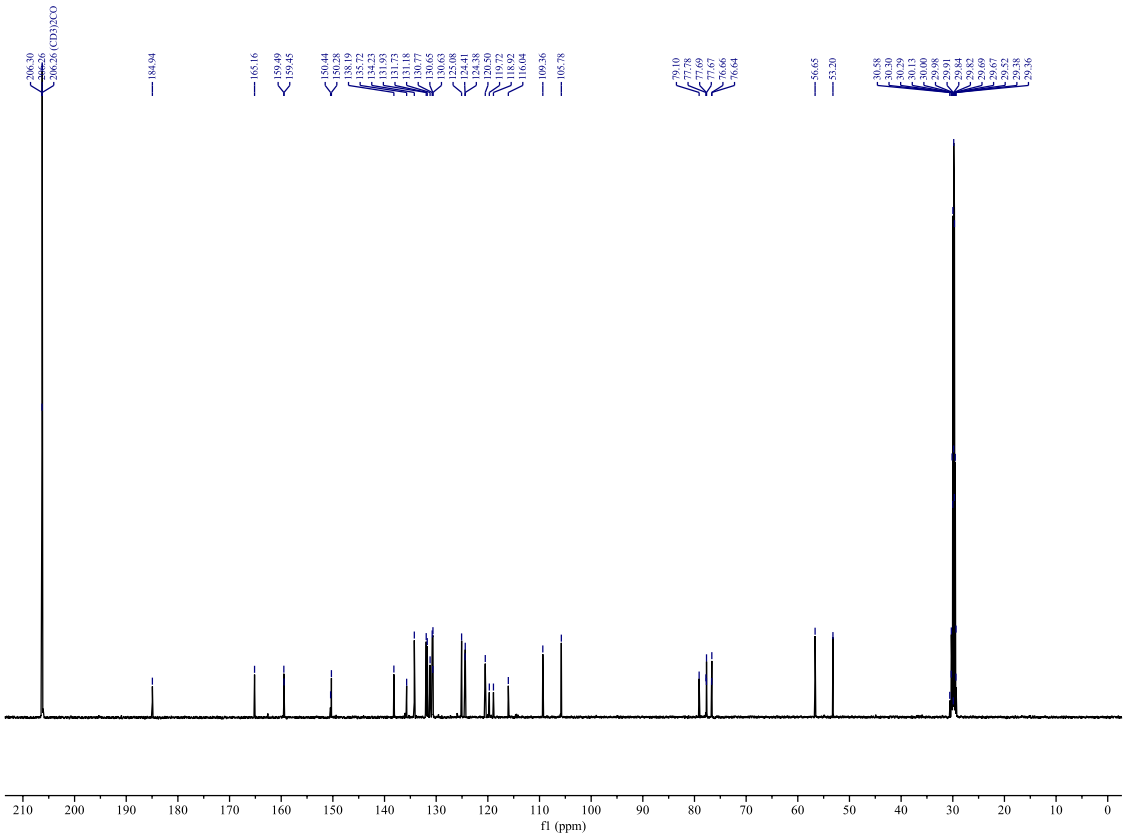

Figure S.8 *^{13}C NMR (126 MHz, $(CD_3)_2CO$) spectrum of DPRP-SNAFL (**2**)*

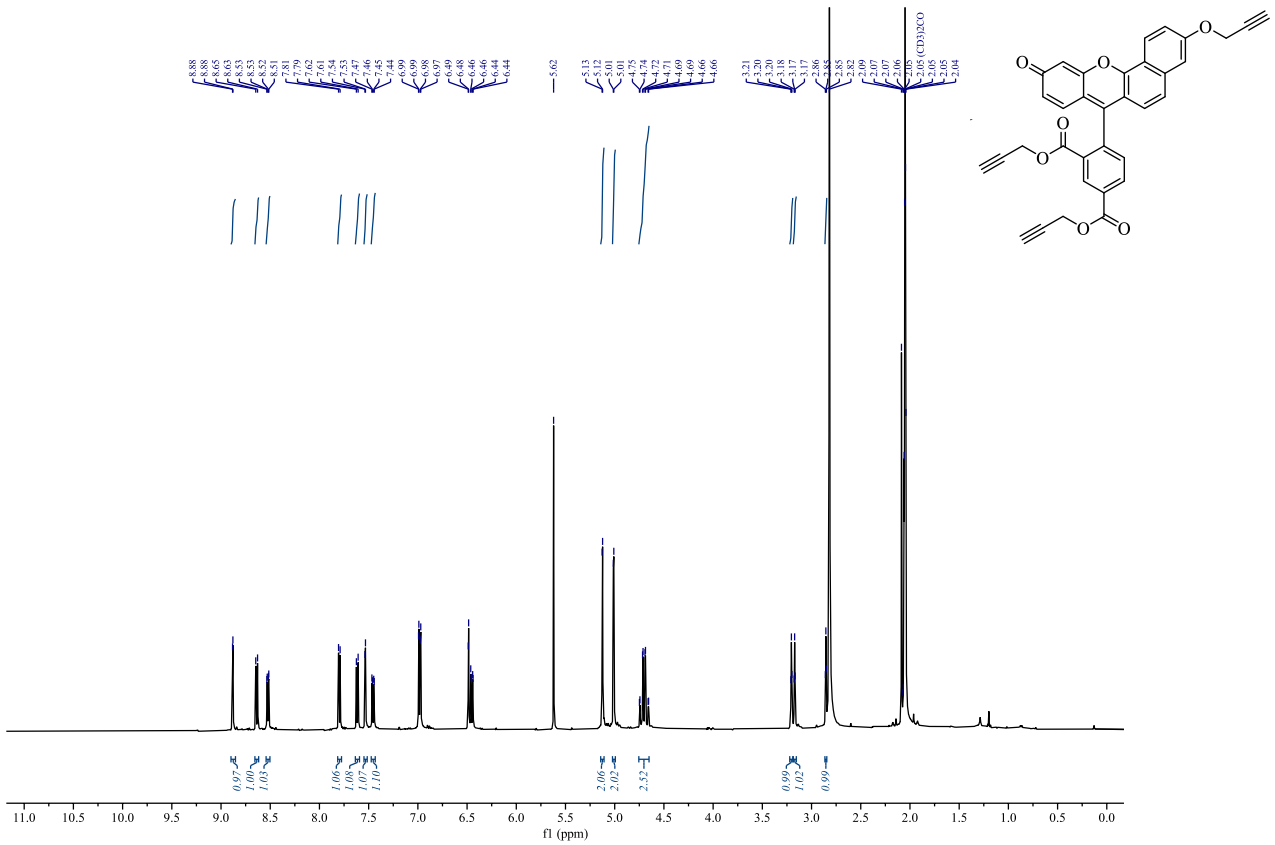

Figure S.9 *^{1}H NMR (500 MHz, $(CD_3)_2CO$) spectrum of TPRP-SNAFL (**1**)*

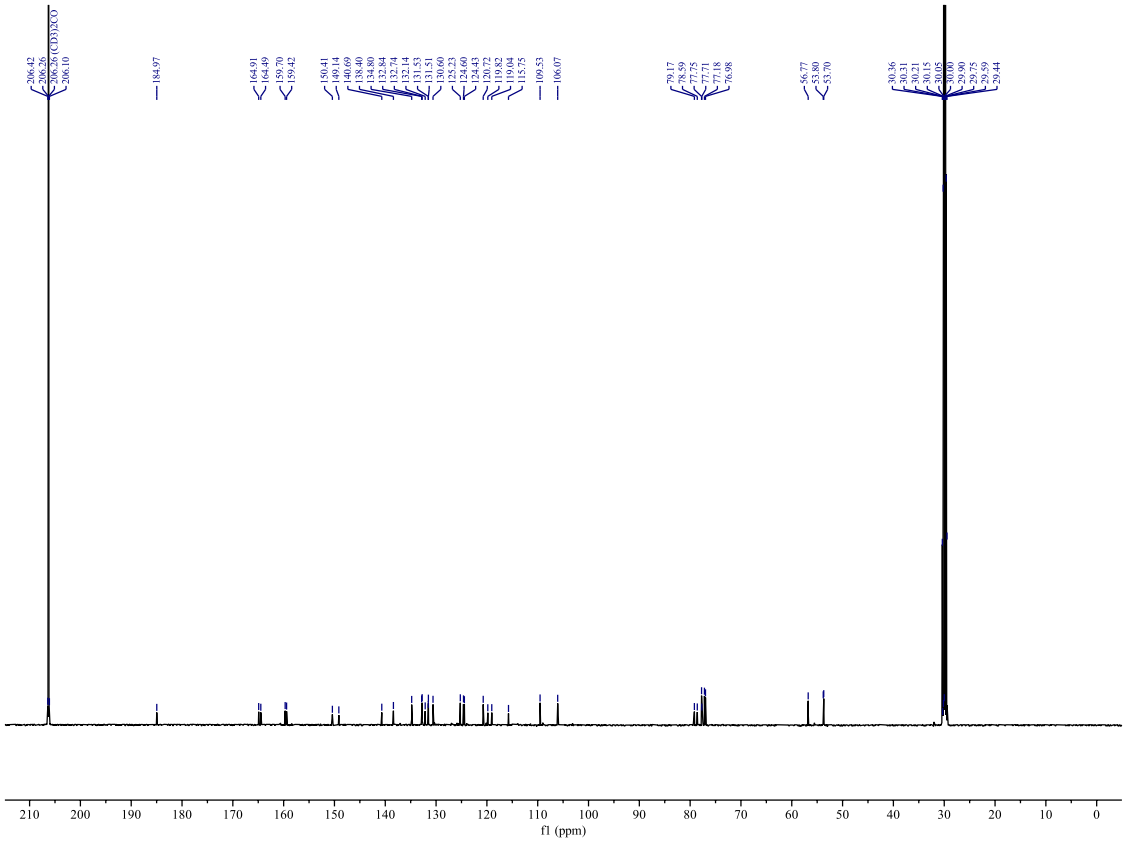

Figure S.10 *^{13}C NMR (126 MHz, $(CD_3)_2CO$) spectrum of TPRP-SNAFL (**1**)*

1.4 Model Thiol-Yne Reaction

The model radical thiol-yne coupling of alkyne DPRP-SNAFL (**2**) and1-propanethiol was carried out directly in NMR tube (diameter 5 mm) with a handheld UV light source (365 nm, placed 20 mm from sample). H NMR spectra between 0 and 3 h of irradiation (reaction time) are shown below in Fig S.11.

Procedure: A glass vial protected from light was charged with 4.0 mg (0.0087 mmol, 1 eq.) of DPRP-SNAFL. 1-Propanethiol (4 µL, 0.043 mmol, 5 eq.) was pipetted into the vial, followed by 500 µL of deuterated dimethyl sulfoxide (DMSO). A 10 mg/mL solution of photo initiator 2,2-dimethoxy-2-phenylacetophenone in d_6-DMSO was prepared, of which 10 µL (0.1 mg, 0.05 eq.) was pipetted into the mixture. The contents of the vial were mixed thoroughly, transferred to an NMR tube in darkness, and affixed horizontally under a UV lamp. Irradiation (365 nm) was carried out in timed intervals at room temperature, with thorough mixing every 30 minutes or less.

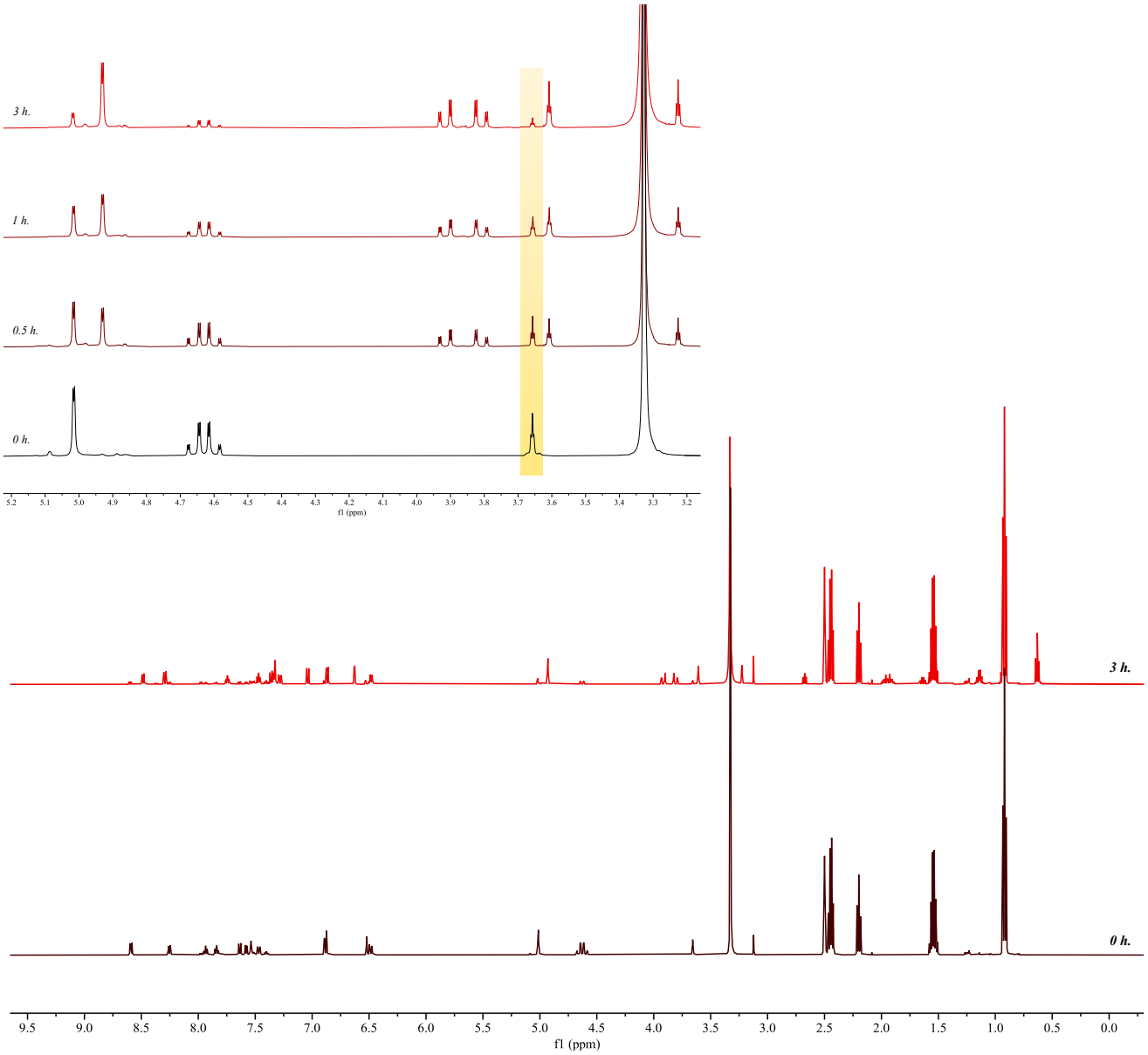

Figure S.11 *^{1}H NMR (500 MHz, d_6-DMSO) spectra illustrating model thiol-yne radical reaction. Primary stacked full spectrum features initial mixture (bottom, 0 h) and final reaction mixture in (top, 3 h irradiation). Inset: Stacked spectra of reaction mixtures at selected time intervals, in 5.2-3.1 ppm region. Disappearance of alkyne signal (3.65 ppm, triplet, 1H) is highlighted. Secondary DPRP-SNAFL alkyne proton obscured by residual water peak at 3.3 ppm.*

2. Spectral & Photophysical Characterization

2.1 Extinction Coefficients

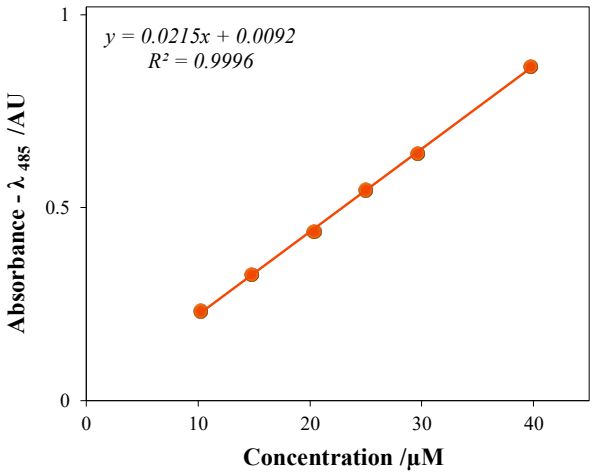

Figure S.12 *Standard curve of TPRP-SNAFL absorbance (λ = 485 nm) in acetone (**1**, dissolved state)*

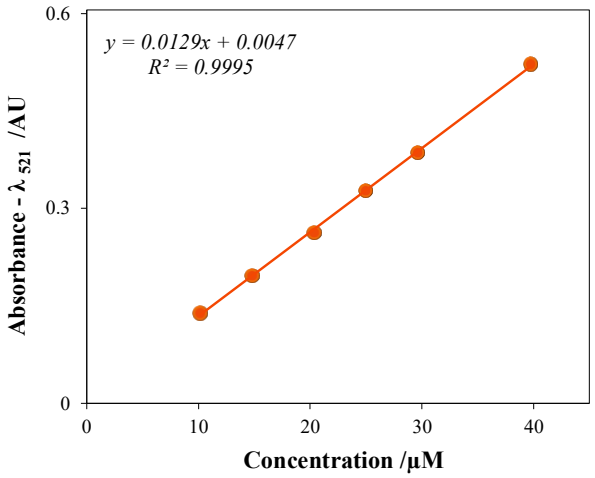

Figure S.13 *Standard curve of TPRP-SNAFL absorbance (λ = 521 nm) in acetone (**1**, dissolved state)*

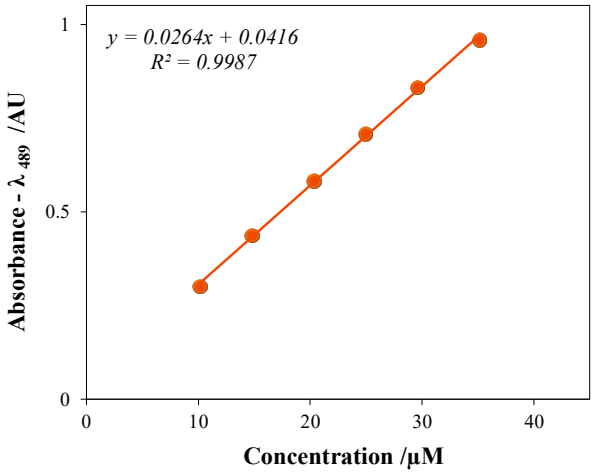

Figure S.14 *Standard curve of TPRP-SNAFL absorbance (λ = 489 nm) in f_w = 70% water/acetone mixture (**1**, aggregated state)*

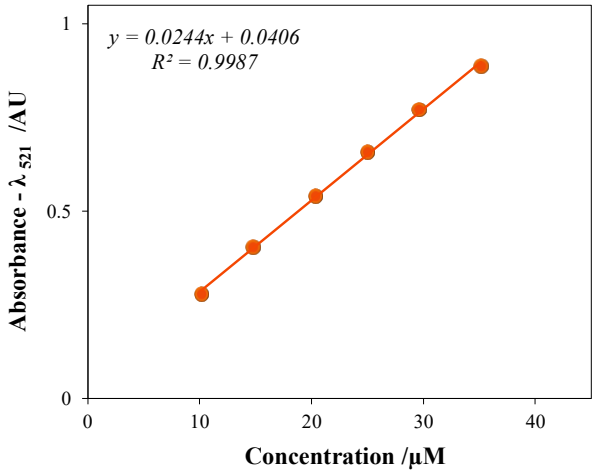

Figure S.15 *Standard curve of TPRP-SNAFL absorbance (λ = 521 nm) in f_w = 70% water/acetone mixture (**1**, aggregated state)*

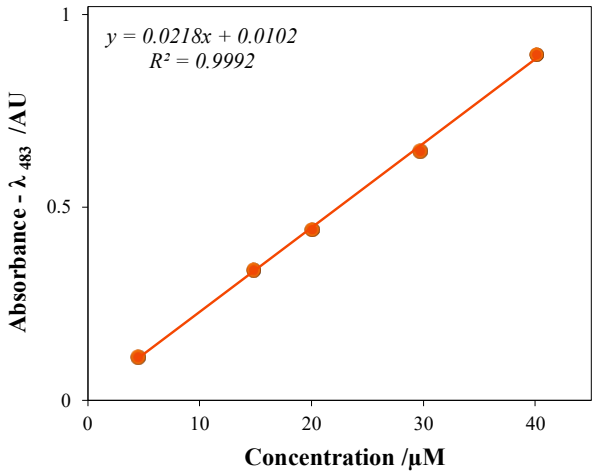

Figure S.16 *Standard curve of DPRP-SNAFL absorbance (λ = 483 nm) in acetone (**2**, dissolved state)*

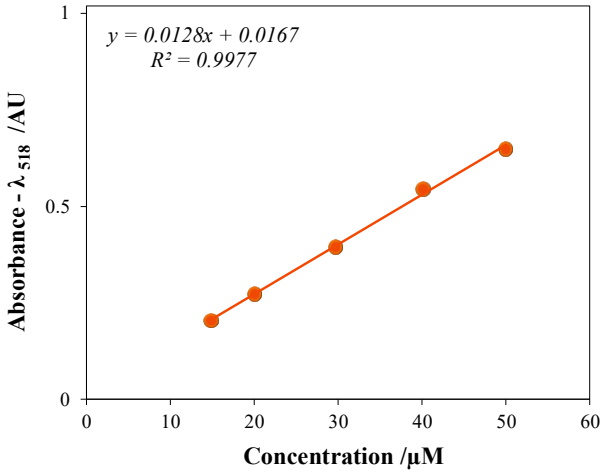

Figure S.17 *Standard curve of DPRP-SNAFL absorbance (λ = 518 nm) in acetone (**2**, dissolved state)*

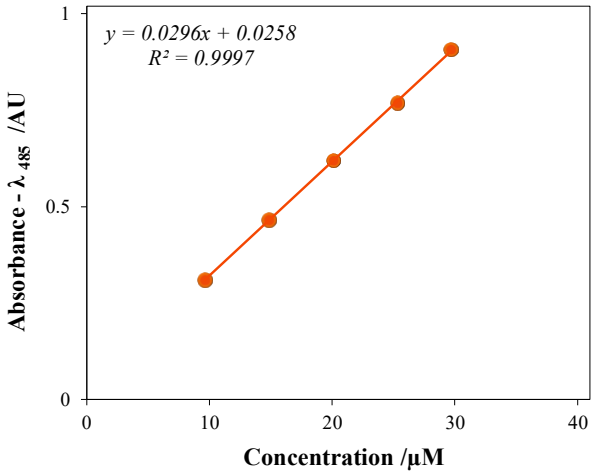

Figure S.18 *Standard curve of DPRP-SNAFL absorbance (λ = 485 nm) in f = 70% water/acetone mixture (**2**, aggregated state)*

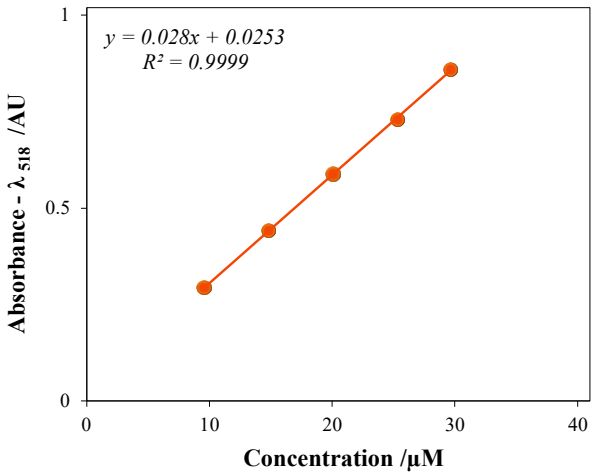

Figure S.19 *Standard curve of DPRP-SNAFL absorbance (λ = 518 nm) in f = 70% water/acetone mixture (**2**, aggregated state)*

2.2 UV-Vis Absorbance Spectra

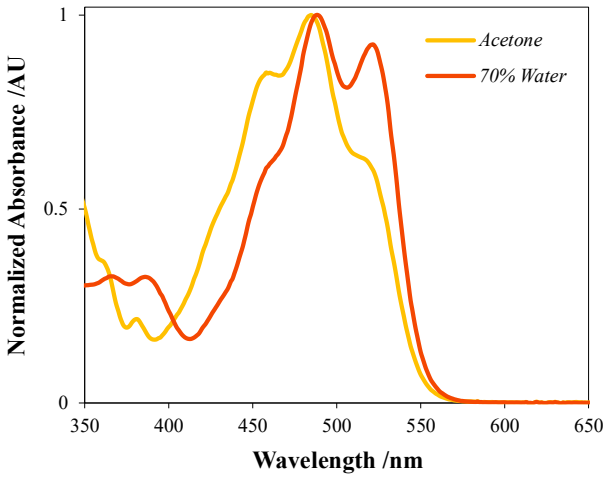

Figure S.20 *Normalized UV-Vis absorbance spectra of **1** dissolved in acetone and aggregated in f_w = 70% acetone/water*

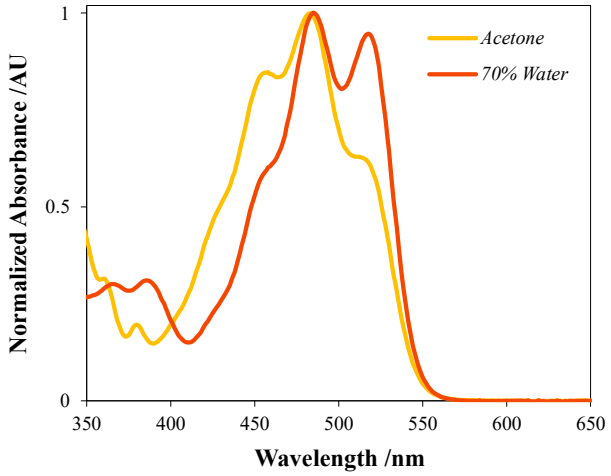

Figure S.21 *Normalized UV-Vis absorbance spectra of* ***2*** *dissolved in acetone and aggregated in* f_w *= 70% acetone/water*

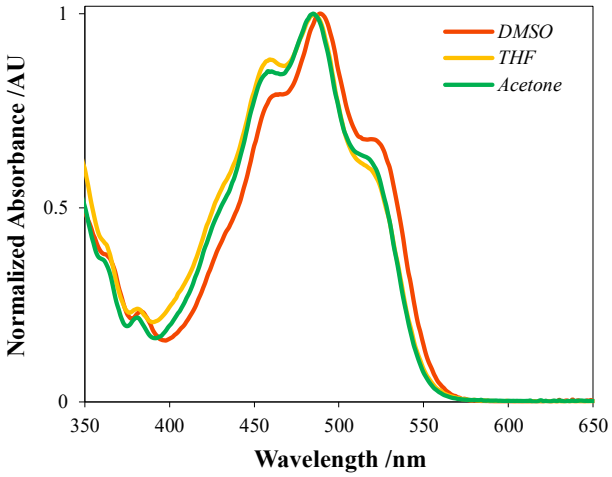

Figure S.22 *Normalized UV-Vis absorbance spectra of* ***1*** *dissolved in aprotic organic solvents*

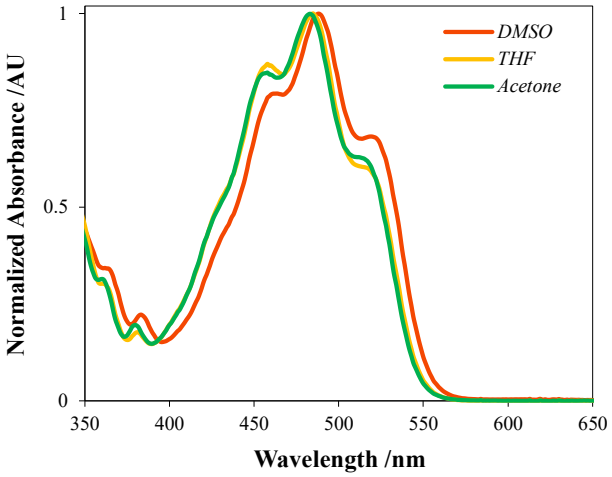

Figure S.23 *Normalized UV-Vis absorbance spectra of* ***2*** *dissolved in aprotic organic solvents*

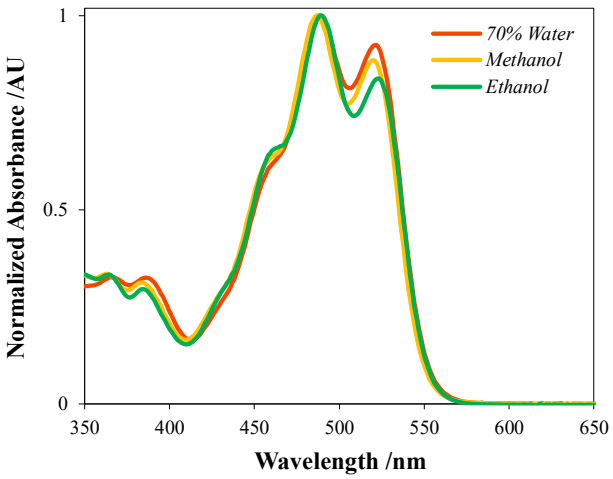

Figure S.24 *Normalized UV-Vis absorbance spectra of* ***1*** *aggregated in polar protic solvents*

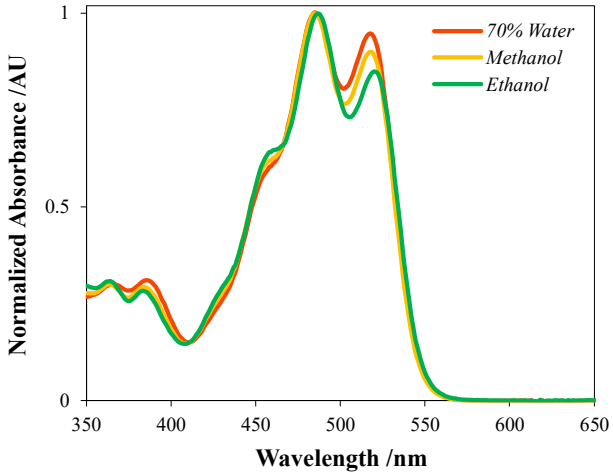

Figure S.25 *Normalized UV-Vis absorbance spectra of* ***2*** *aggregated in polar protic solvents*

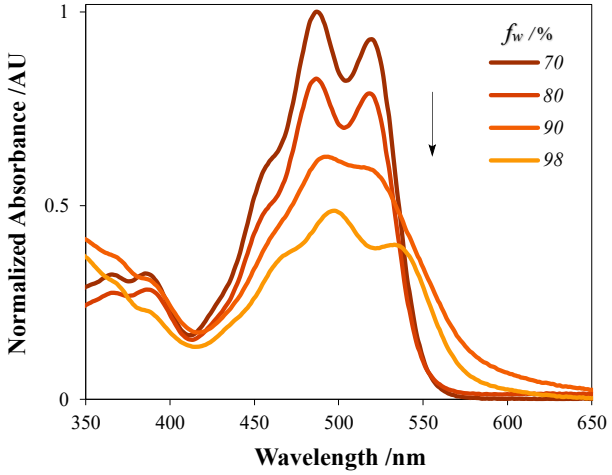

Figure S.26 *Normalized UV-Vis absorbance spectra of* ***1*** *in acetone/aqueous binary mixtures of varying water content, at and above the 'cutoff point' of 70% v/v*

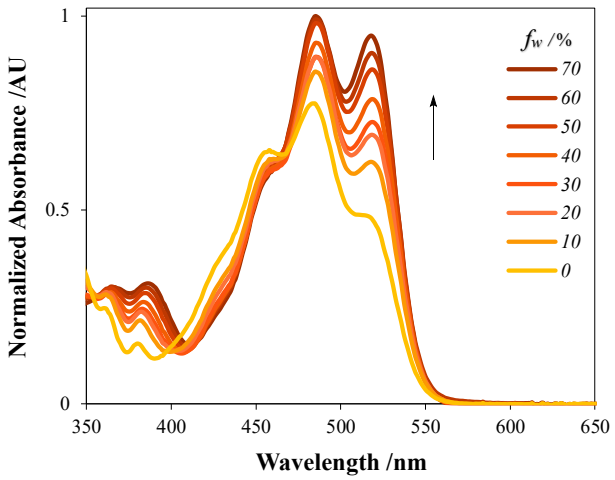

Figure S.27 *Normalized UV-Vis absorbance spectra of* ***2*** *in acetone/aqueous binary mixtures of varying water content (0-70% v/v)*

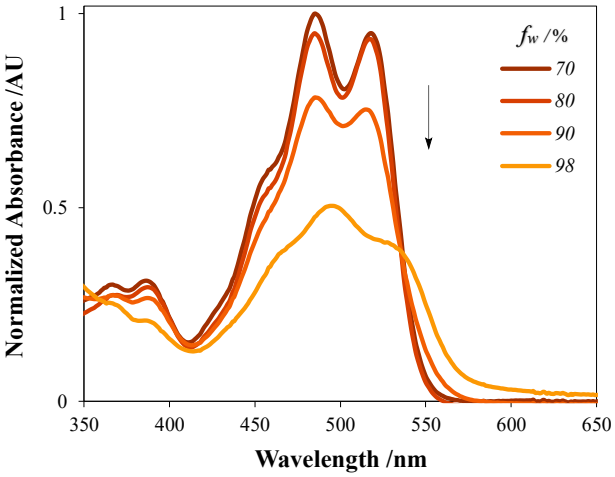

Figure S.28 *Normalized UV-Vis absorbance spectra of* ***2*** *in acetone/aqueous binary mixtures of varying water content, at and above the 'cutoff point' of 70% v/v*

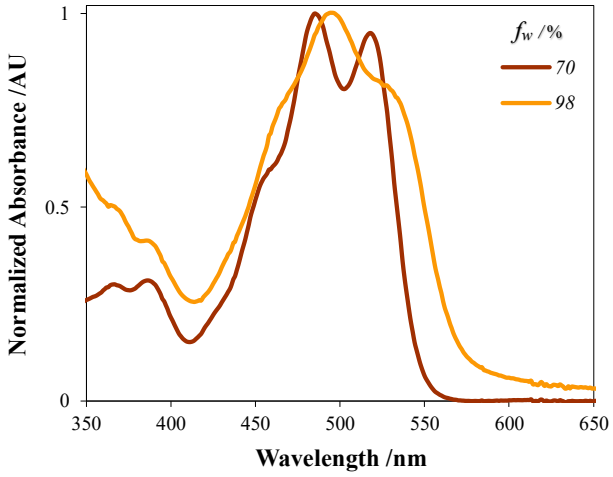

Figure S.29 *Comparative normalized UV-Vis absorbance spectra of* ***2*** *at maximum absorbance of 70% v/v and minimum of 98% v/v*

2.3 Fluorescence Emission Spectra

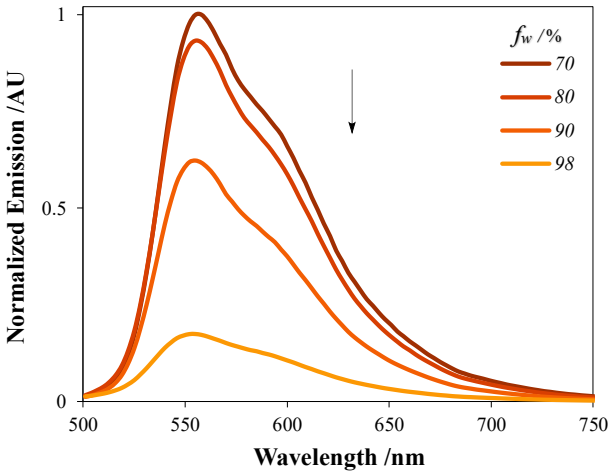

Figure S.30 *Normalized emission spectra of* ***1*** *in acetone/aqueous binary mixtures of varying water content, at and above the 'cutoff point' of 70% w/w*

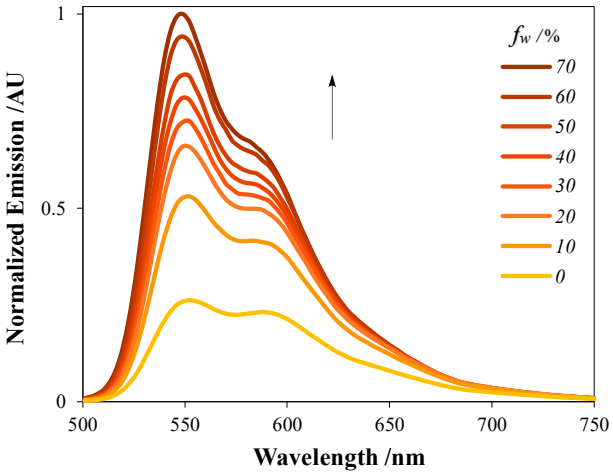

Figure S.31 *Normalized emission spectra of* ***2*** *in acetone/aqueous binary mixtures of varying water content*

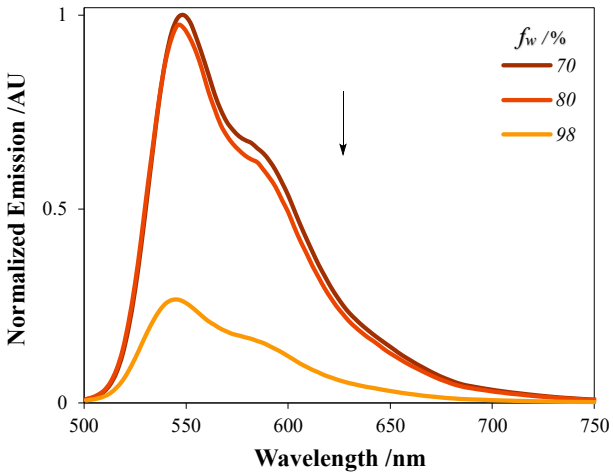

Figure S.32 *Normalized emission spectra of* ***2*** *in acetone/aqueous binary mixtures of varying water content, at and above the 'cutoff point' of 70% w/w*

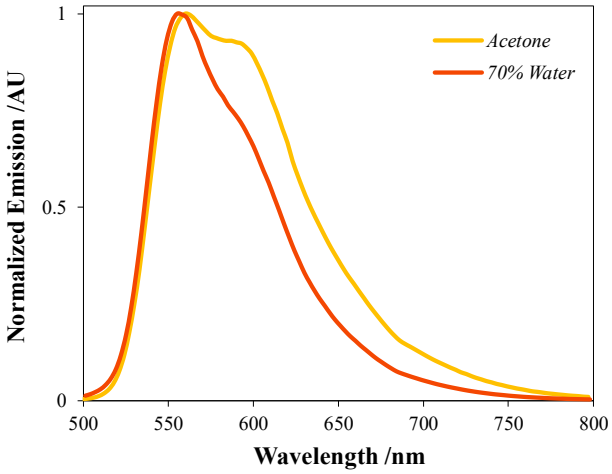

Figure S.33 *Normalized emission spectra of* ***1*** *dissolved in acetone and aggregated in* f_w *= 70% acetone/water*

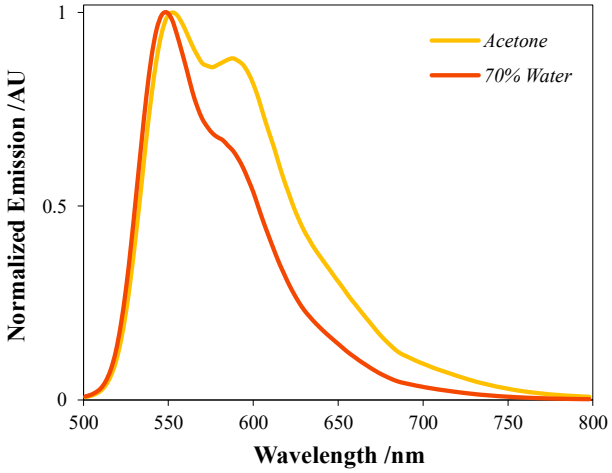

Figure S.34 *Normalized emission spectra of* ***2*** *dissolved in acetone and aggregated in* f_w *= 70% acetone/water*

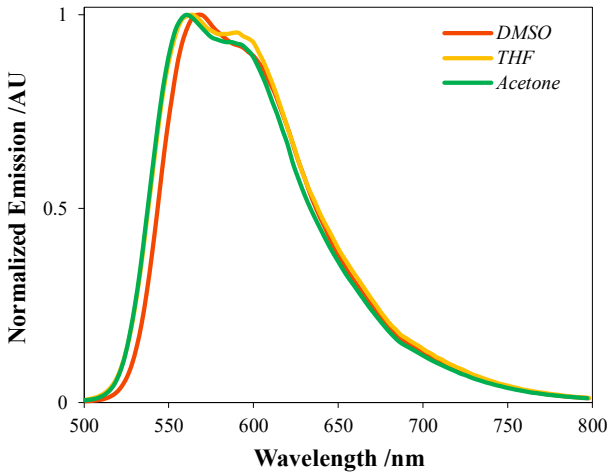

Figure S.35 *Normalized emission spectra of* ***1*** *dissolved in selected aprotic organic solvents*

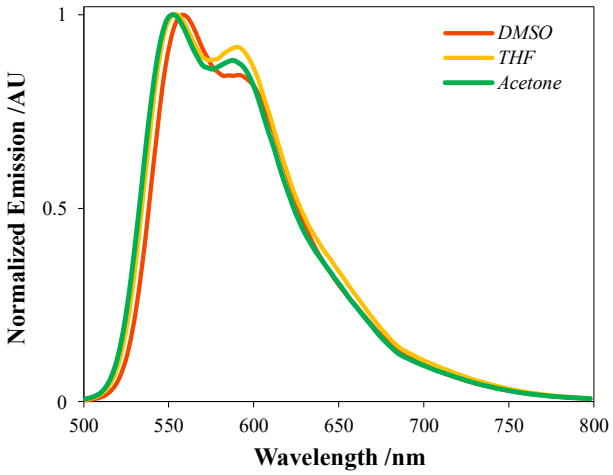

Figure S.36 *Normalized emission spectra of* ***2*** *dissolved in selected aprotic organic solvents*

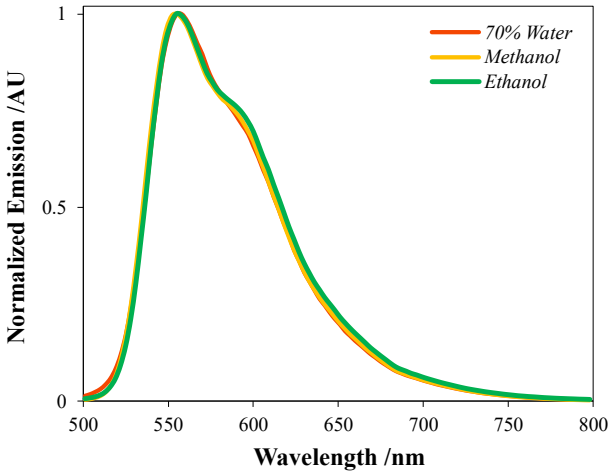

Figure S.37 *Normalized emission spectra of* ***1*** *aggregated in polar protic solvents*

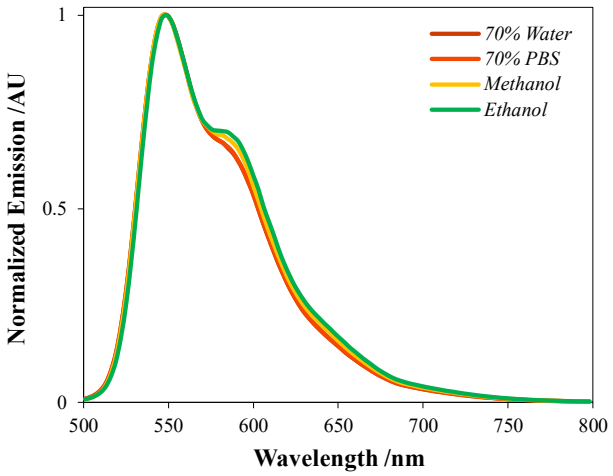

Figure S.38 *Normalized emission spectra of* ***2*** *aggregated in polar protic solvents*

2.4 Miscellaneous

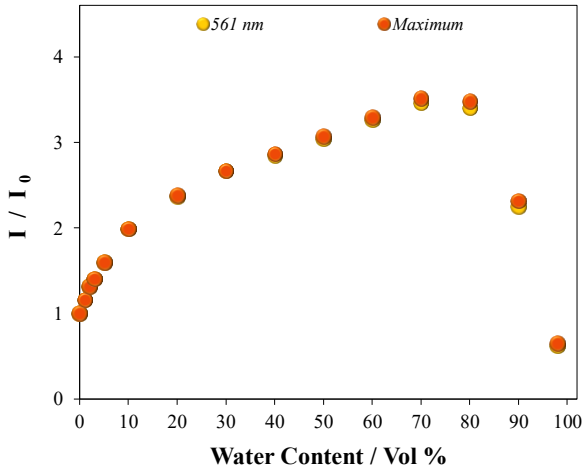

Figure S.39 *Relative fluorescence intensity of* ***1*** *with varying water fraction normalized to emission in pure acetone, with monitoring at a fixed wavelength of 561 nm and at maximum intensity*

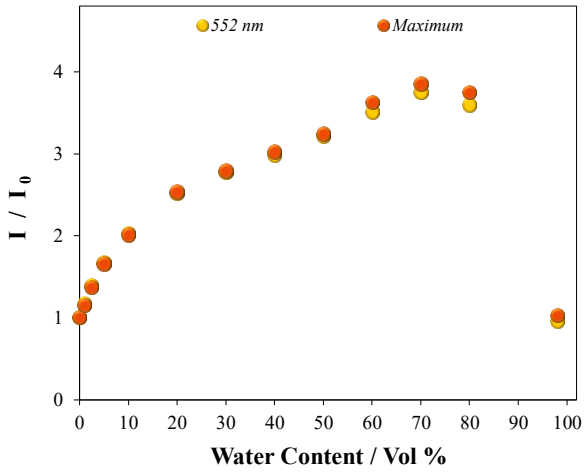

Figure S.40 *Relative fluorescence intensity of* ***2*** *with varying water fraction normalized to emission in pure acetone, with monitoring at a fixed wavelength of 552 nm and at maximum intensity*

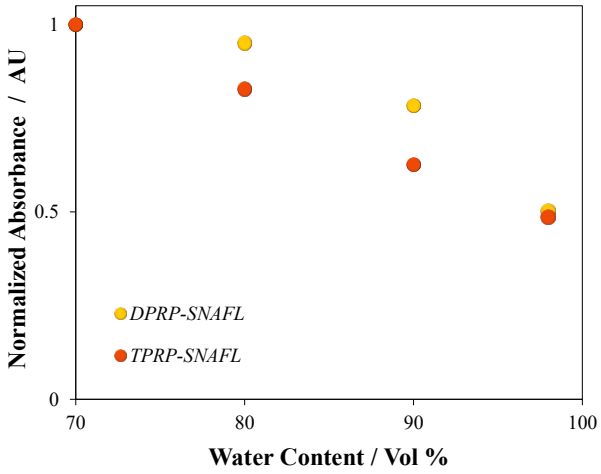

Figure S.41 *Visualized normalized absorbance of* ***1*** *and* ***2*** *(monitored at maximum) at and above the cutoff point of 70% w/w*

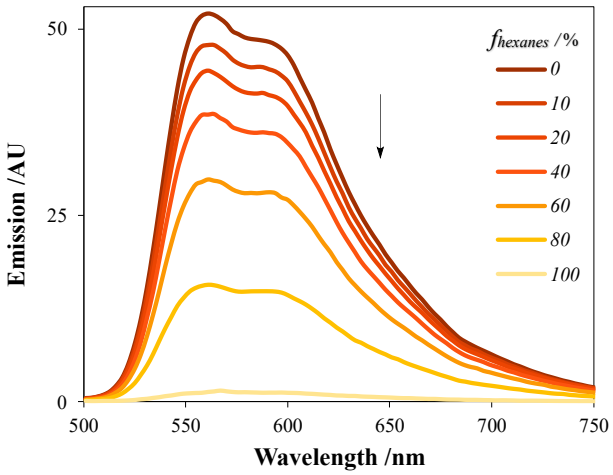

Figure S.42 *Emission spectra of* ***1*** *in binary solutions of acetone/hexanes with varying hexanes content*

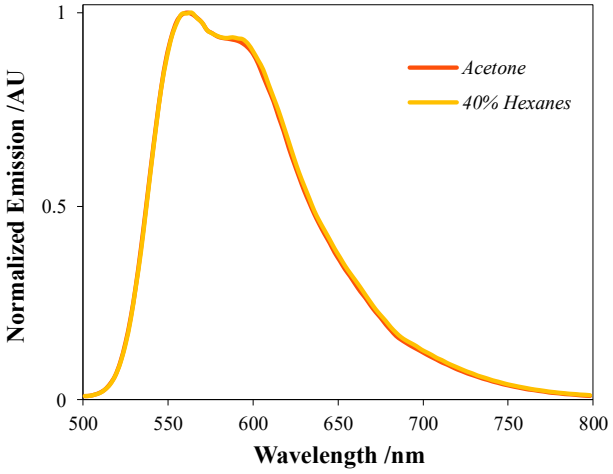

Figure S.43 *Normalized emission spectra of* ***1*** *in pure acetone and a binary solution of acetone/hexanes (*$f_{hexanes}$ *= 40%)*

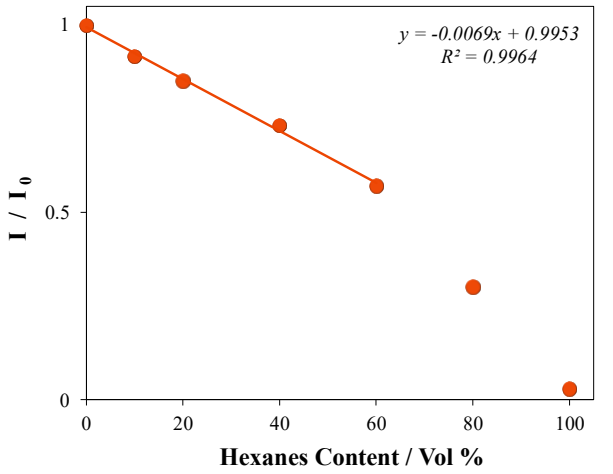

Figure S.44 *Relative fluorescence intensity of* ***1*** *in acetone/hexanes binary mixtures of varying hexanes content by volume, normalized to emission in pure acetone. Linear fit shown for 0-60% hexanes.*

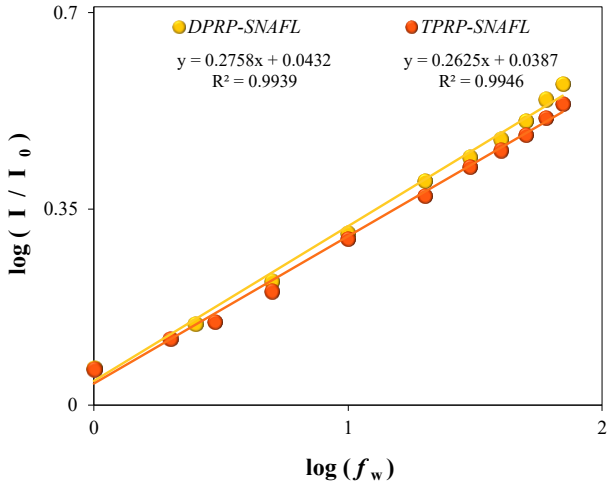

Figure S.45 *Quantification of water content in acetone with compounds* ***1*** *and* ***2*** *via emission enhancement ratio I / I₀ over broader range of reasonable linearity (1-70%)*

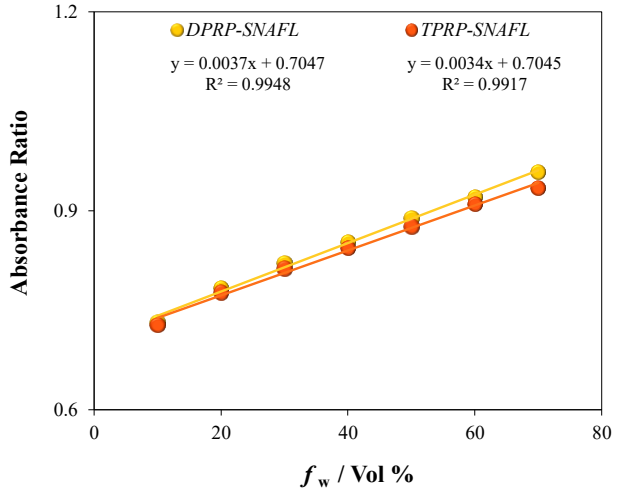

Figure S.46 *Quantification of water content in acetone with compounds* ***1*** *and* ***2*** *via absorbance ratio (****1*** *- Abs 521/485 nm,* ***2*** *- Abs 518/483 nm) over broader range of reasonable linearity (10-70%)*

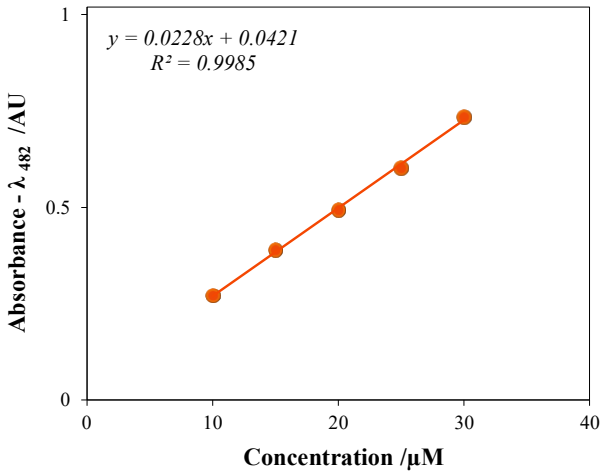

Figure S.47 *Standard curve of SNAFL absorbance (λ = 482 nm) in pH 6.0 PBS buffer (****I-2****, neutral/naphthol state)*

Table S.1 *Comparison of selected optical properties for luminogens and their SNAFL precursors*

Compound	*Solvent*	λ_{abs} /nm	ε_{λ} /$M^{-1}cm^{-1}$	λ_{em} /nm
TPRP-SNAFL	Acetone	485	21,500	561
DPRP-SNAFL	Acetone	483	21,800	552
Carboxy-SNAFL (Naphthol)[1]	PBS Buffer (pH 6.0)	485	26,400	543
SNAFL (Naphthol)	PBS Buffer (pH 6.0)	482	22,800	541

Table S.2 *Calculation of full width half maximum (FWHM) values.*

Compound	*Solvent (State)*	λ_{em-0} /nm	λ_{em-1} /nm	λ_{em-2} /nm	*FWHM* /nm
TPRP-SNAFL	Acetone (Dissolved)	560	539	635	96
DPRP-SNAFL	Acetone (Dissolved)	552	534	624	90
TPRP-SNAFL	70% Water/Acetone (Aggregates)	555	537	615	78
DPRP-SNAFL	70% Water/Acetone (Aggregates)	549	531	603	72

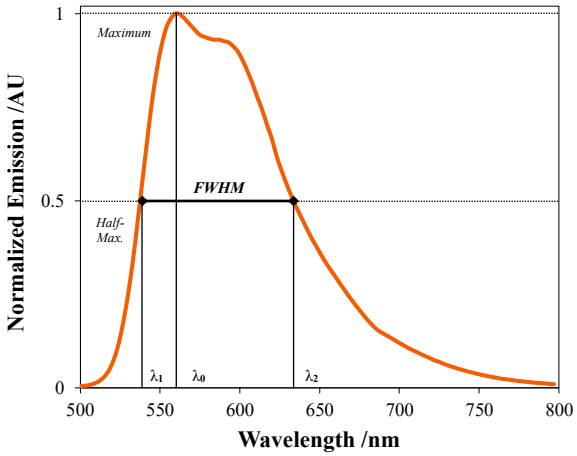

Figure S.48 *Calculation of full width half maximum (FWHM = λ_{em-2} - λ_{em-1}) visualized on emission spectrum of TPRP-SNAFL in acetone*

Figure S.49 *Appearance of DPRP-SNAFL. Left: In solution (20 µM in acetone) under ambient light. Right: Adsorbed on silica TLC plate illuminated by 365 nm light source.*

2.5 Quantum Yields

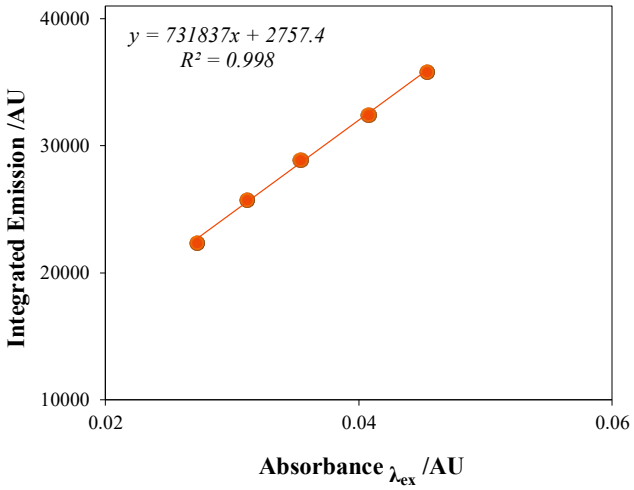

Figure S.50 *Quantum yield determination of standard rhodamine 101 (inner salt) in ethanol (λ_{ex} = 540 nm)*

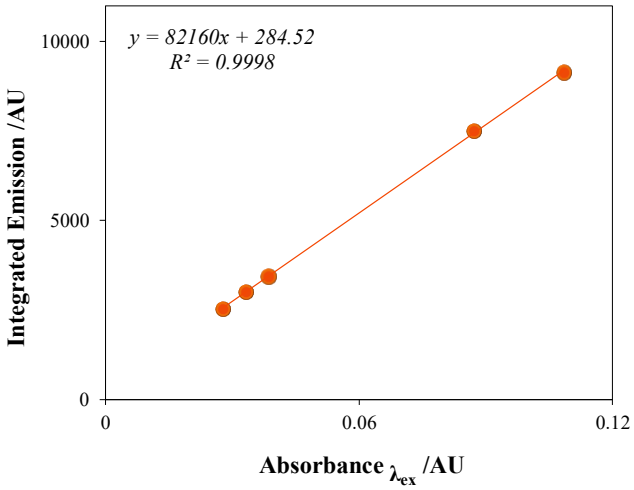

Figure S.51 *Quantum yield determination of* ***1*** *dissolved in acetone (λ_{ex} = 485 nm)*

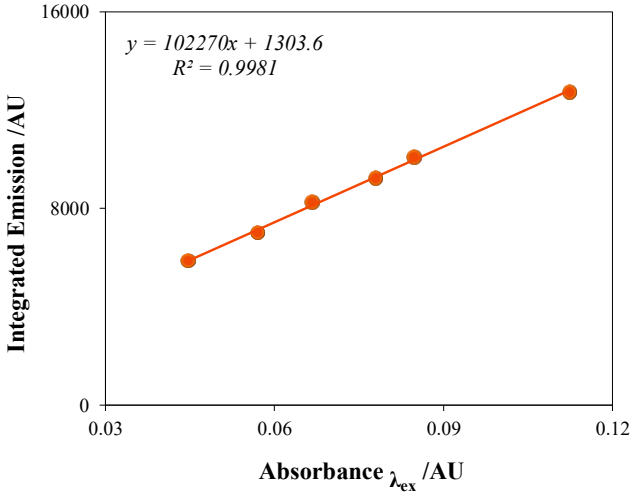

Figure S.52 *Quantum yield determination of* ***2*** *dissolved in acetone (λ_{ex} = 485 nm)*

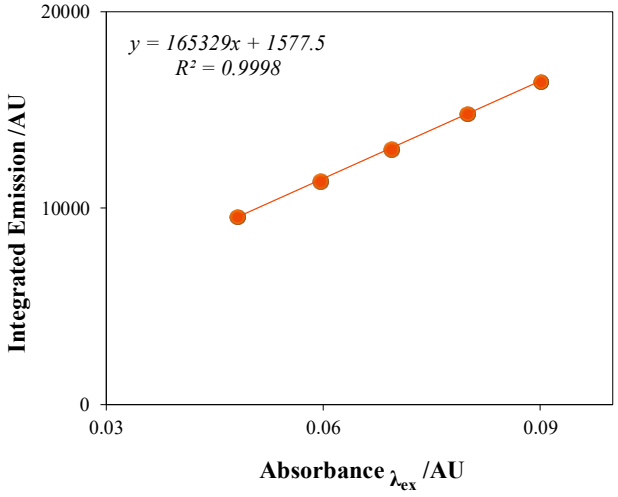

Figure S.53 *Quantum yield determination of* ***1*** *aggregated in acetone/water at 70% v/v (λ_{ex} = 485 nm)*

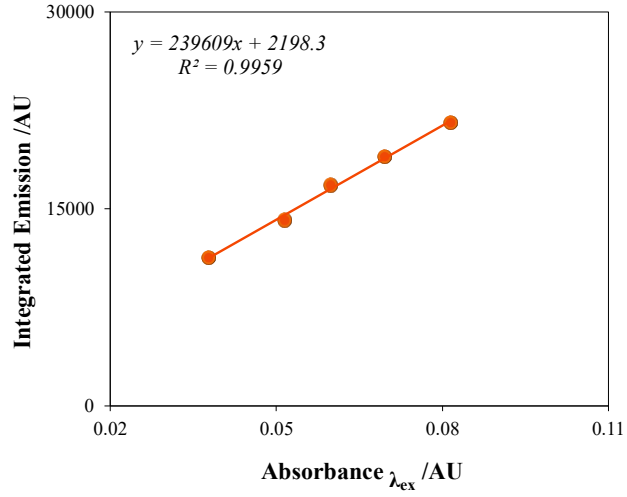

Figure S.54 *Quantum yield determination of* ***2*** *aggregated in acetone/water at 70% v/v (λ_{ex} = 485 nm)*

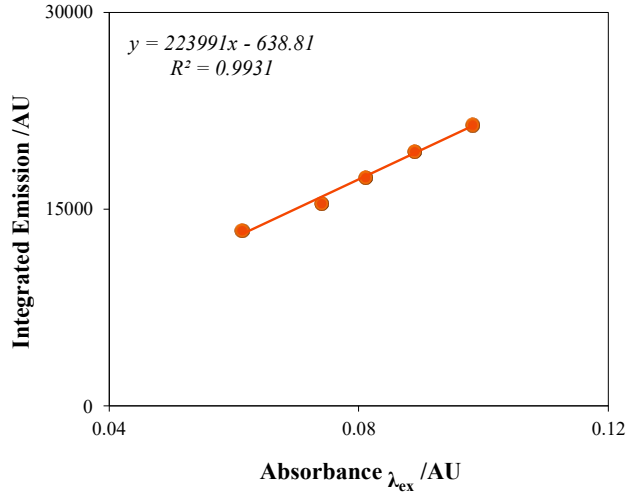

Figure S.55 *Quantum yield determination of* ***1*** *aggregated in methanol (λ_{ex} = 485 nm)*

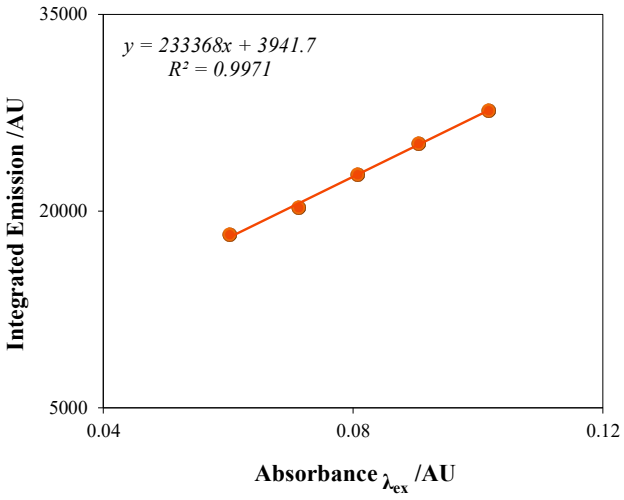

Figure S.56 *Quantum yield determination of* ***2*** *aggregated in methanol (λ_{ex} = 485 nm)*

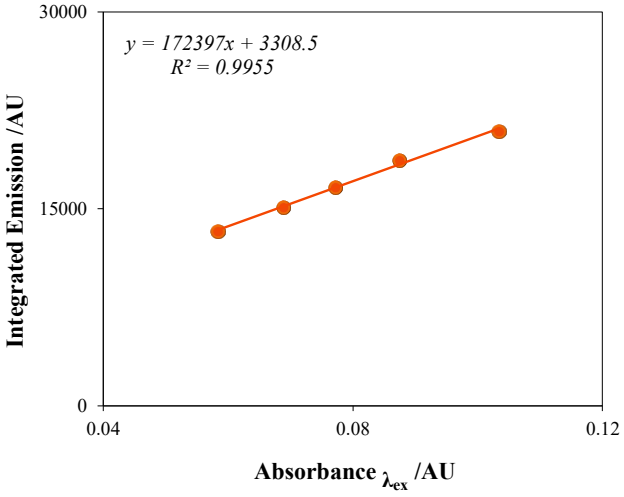

Figure S.57 *Quantum yield determination of* ***1*** *aggregated in ethanol (λ_{ex} = 485 nm)*

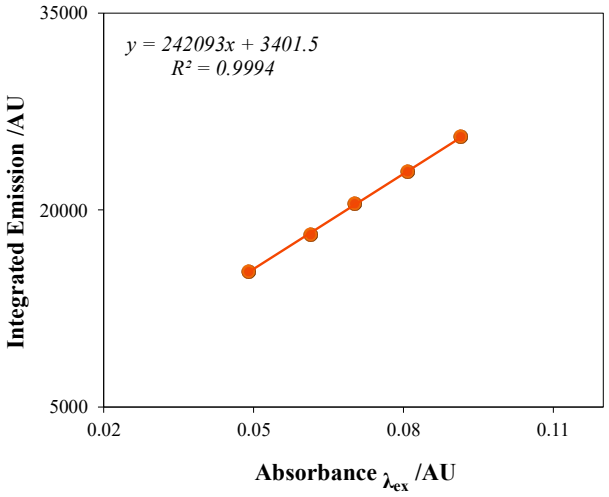

Figure S.58 *Quantum yield determination of* ***2*** *aggregated in ethanol (λ_{ex} = 485 nm)*

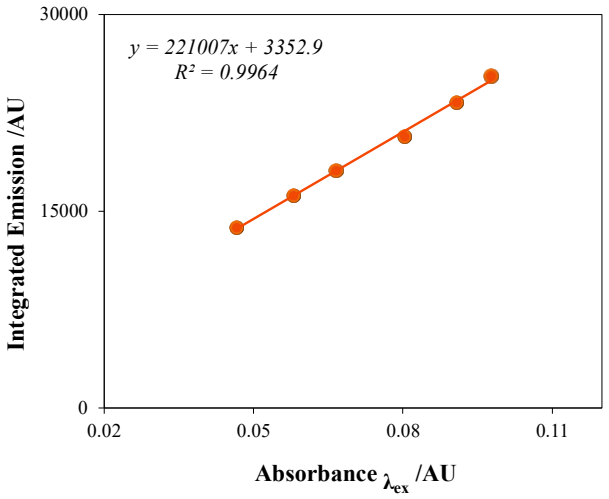

Figure S.59 *Quantum yield determination of* ***2*** *aggregated in acetone/PBS buffer at 70% v/v (λ_{ex} = 485 nm)*

Table S.3 *Summary of data relevant to quantum yield determinations*

Species	***Slope***	***R^2***	***Refractive Index***	***Φ_f***
Rhodamine 101 *(Ethanol)*	731837 (732000 ± 19000)	0.9980	1.3660	0.98 ± 0.09 [2]
TPRP-SNAFL *(Acetone)*	82160 (82200 ± 700)	0.9998	1.3586 [3]	0.11 ± 0.01
DPRP-SNAFL *(Acetone)*	102270 (102300 ± 2200)	0.9981	1.3586	0.14 ± 0.01
TPRP-SNAFL *(Acetone/ Water, f_w = 70%)*	165329 165300 ±1400	0.9998	1.3540 [3]	0.22 ± 0.02
DPRP-SNAFL *(Acetone/ Water, f_w = 70%)*	239609 240000 ± 9000	0.9959	1.3540	0.32 ± 0.03
DPRP-SNAFL *(Acetone/ PBS, f_w = 70%)*	221007 221000 ± 7000	0.9964	1.3540	0.29 ± 0.03
TPRP-SNAFL *(Methanol)*	223991 224000 ± 600	0.9931	1.3309 [4]	0.28 ± 0.03
DPRP-SNAFL *(Methanol)*	233368 233000 ± 7000	0.9971	1.3309	0.30 ± 0.03
TPRP-SNAFL *(Ethanol)*	172397.0502 172000 ± 7000	0.9955	1.3660 [4]	0.23 ± 0.03
DPRP-SNAFL *(Ethanol)*	242093 242000 ± 3000	0.9994	1.3660	0.32 ± 0.03

2.6 Fluorescence Lifetimes

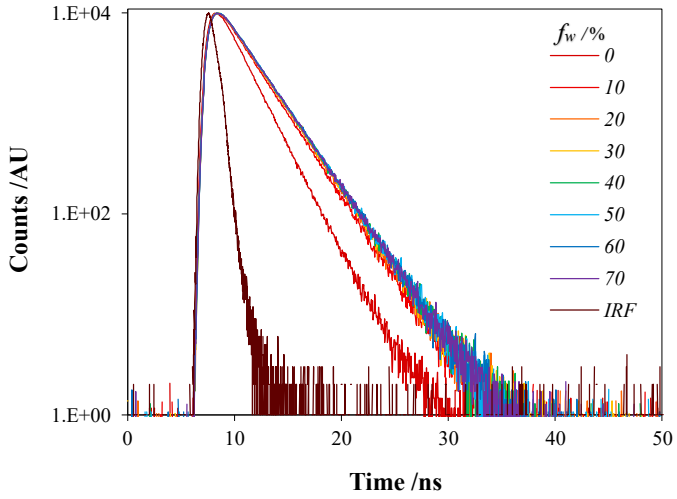

Figure S.60 *Time resolved fluorescence emission decay of* ***1*** *in binary acetone/water solutions of varying water content, with instrument response factor (IRF) illustrated*

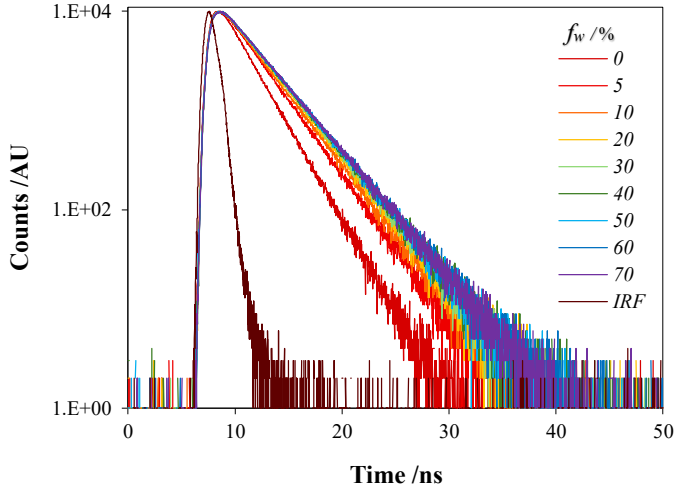

Figure S.61 *Time resolved fluorescence emission decay of* ***2*** *in binary acetone/water solutions of varying water content, with instrument response factor (IRF) illustrated*

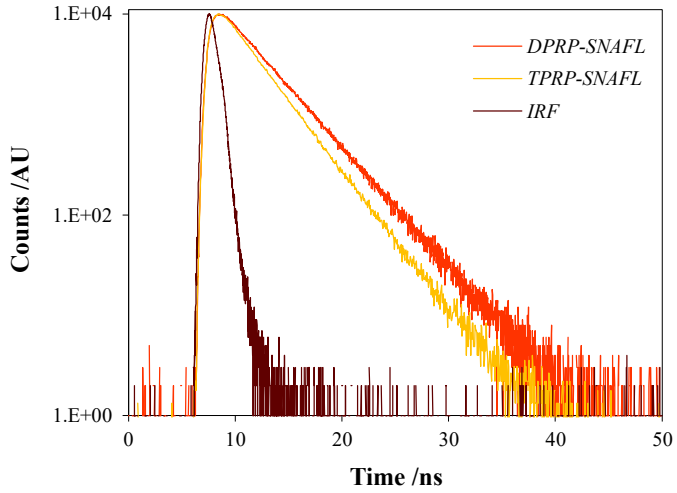

Figure S.62 *Time resolved fluorescence emission decay of* ***1*** *and* ***2*** *in methanol, with instrument response factor (IRF) illustrated*

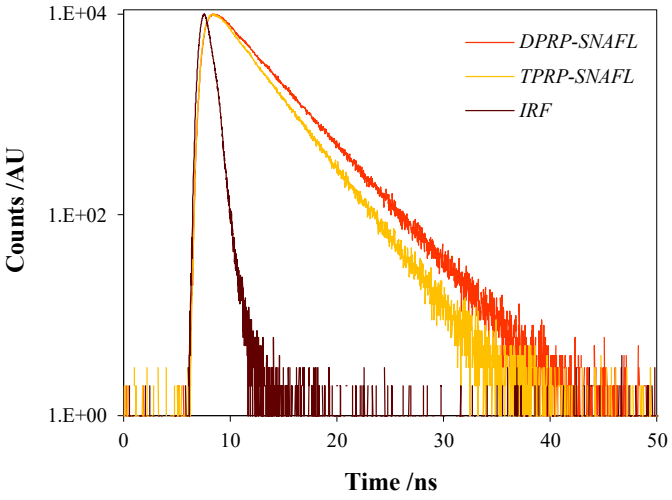

Figure S.63 *Time resolved fluorescence emission decay of **1** and **2** in ethanol, with instrument response factor (IRF) illustrated*

3. Crystallography

Table S.4 *Crystallographic parameters for 3-propargyloxy-7-(2,4-di(propargylester)phenyl)-xanth-10-one· $(CH_3)_2C=O$ (TPRP-SNAFL)*

CCDC number	2496456
Empirical formula	$C_{37}H_{26}O_8$
Formula weight	598.58
Temperature/K	80
Crystal system	Triclinic
Space group	P-1
a/Å	9.689(10)
b/Å	12.113(12)
c/Å	13.682(14)
α/°	108.425(10)
β/°	93.040(11)
γ/°	102.406(11)
Volume/Å^3	1475(3)
Z	2
ρ_{calc}g/cm^3	1.348
μ/mm^{-1}	0.095
F(000)	624.0
Crystal size/mm^3	0.4 × 0.09 × 0.03
Radiation	MoKα (λ = 0.71073)
2Θ range for data collection/°	5.582 to 42.694
Index ranges	$-9 \le h \le 9$, $-12 \le k \le 12$, $-13 \le l \le 13$
Reflections collected	7595
Independent reflections	3139 [R_{int} = 0.1663, R_{sigma} = 0.1473]
Data completeness/%	94.3
Data/restraints/parameters	3139/0/408
Goodness-of-fit on F^2	0.958
Final R indexes [I>=2σ (I)]	R_1 = 0.0551, wR_2 = 0.1242
Final R indexes [all data]	R_1 = 0.0916, wR_2 = 0.1488
Largest diff. peak/hole / e Å^{-3}	0.26/-0.26

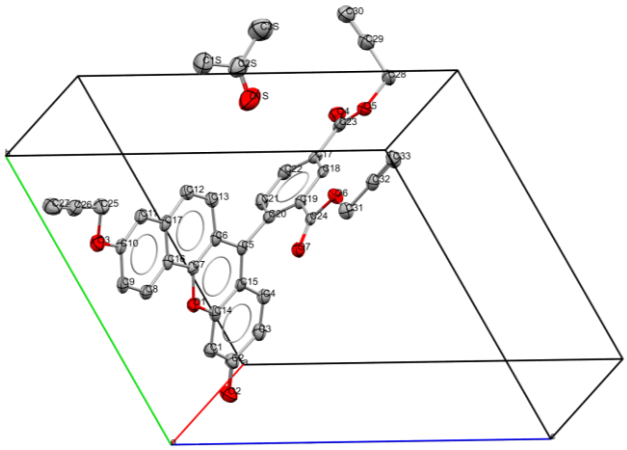

Figure S.64 *Asymmetric unit of 3-propargyloxy-7-(2,4-di(propargylester)phenyl)-xanth-10-one·$(CH_3)_2C=O$ (collected at 80K). Unit cell axes and atomic labelling scheme shown, displacement ellipsoids rendered at the 50% probability level, with hydrogens omitted for clarity*

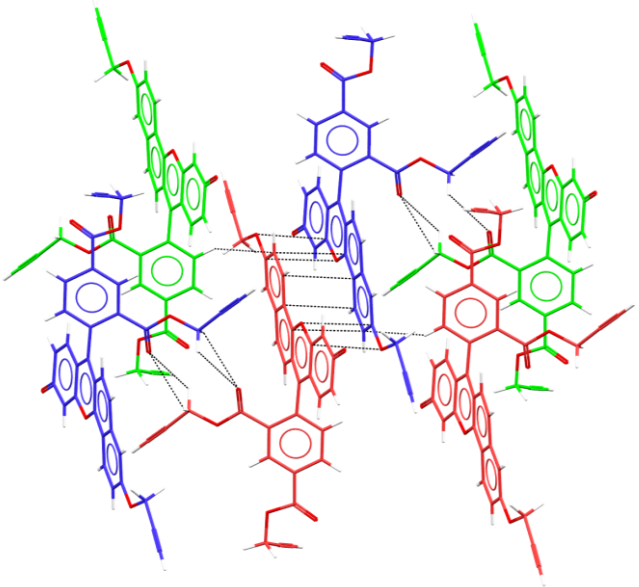

Figure S.65 *View down the crystallographic -b axis of the crystal structure of TPRP-SNAFL. Custom carbon colours are used to show contrast between subunits, and solvated acetone molecules are omitted for clarity. Short contacts between TPRP-SNAFL molecules are shown.*

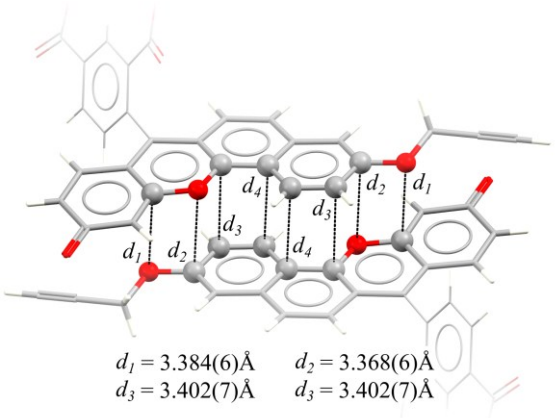

Figure S.66 *Cropped view of C – C distances between π- systems of neighbouring molecules. Nearest neighbour atoms are highlighted with a ball-and-stick model, with capped sticks highlighting the main π- system. The peripheral of the atom was rendered with a wireframe and cropped for clarity*

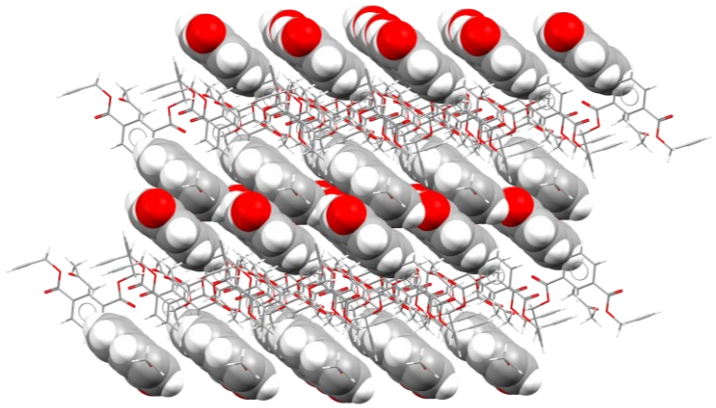

Figure S.67 *View of packed TPRP-SNAFL lattice. Solvated acetone is depicted with a spacefill render, while TPRP-SNAFL molecules are drawn using a capped stick depiction.*

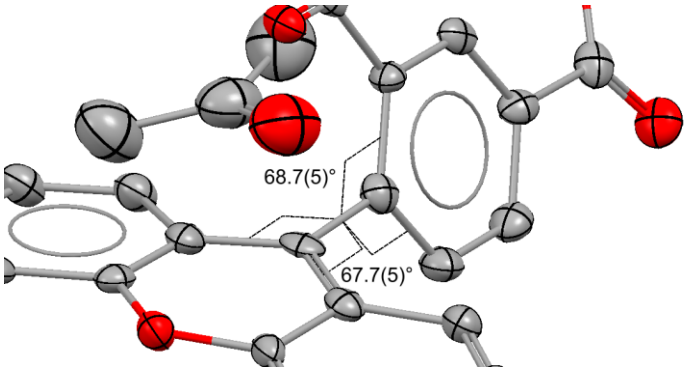

Figure S.68 *Torsion angle of TPRP-SNAFL phenyl substituent. Opposite torsion angles are inequivalent due to slight twist of the xanthenone unit. Atoms are rendered as 50% probability displacement ellipsoids, and hydrogen atoms are omitted from the render for clarity.*

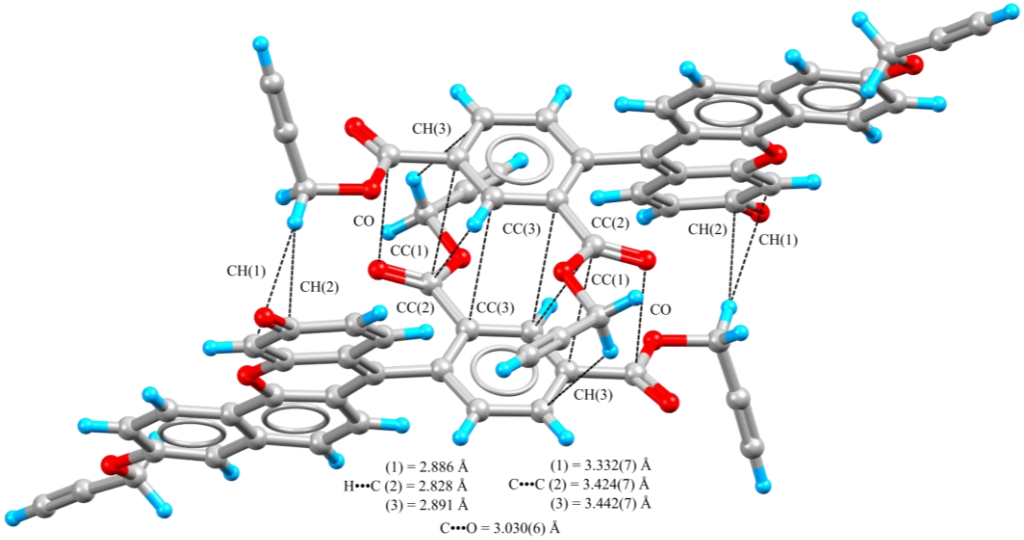

Figure S.69 *View of dimer consisting of TPRP-SNAFL phenyl group edge-to-edge stacking. All short contacts between rendered molecules are depicted, using dashed lines. Atoms are rendered with a ball and stick depiction. Hydrogen positions are simulated as riding on their substituent, thus standard deviations are not determined for hydrogen bonds.*

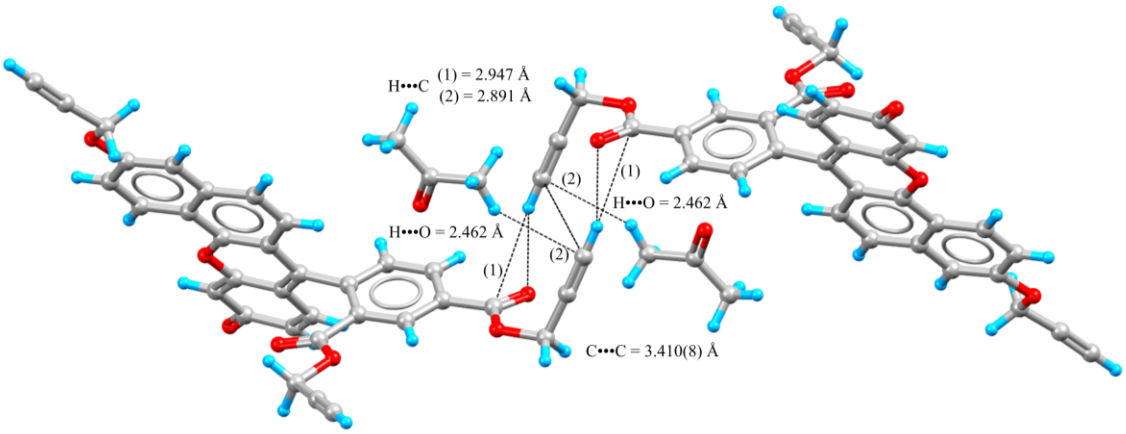

Figure S.70 *View of propargyl dimers on phenyl group of TPRP-SNAFL showing interatomic distances. All short contacts between rendered molecules are depicted, using dashed lines. Atoms are rendered with a ball and stick depiction. Hydrogen positions are simulated as riding on their substituent, thus standard deviations are not determined for hydrogen bonds.*

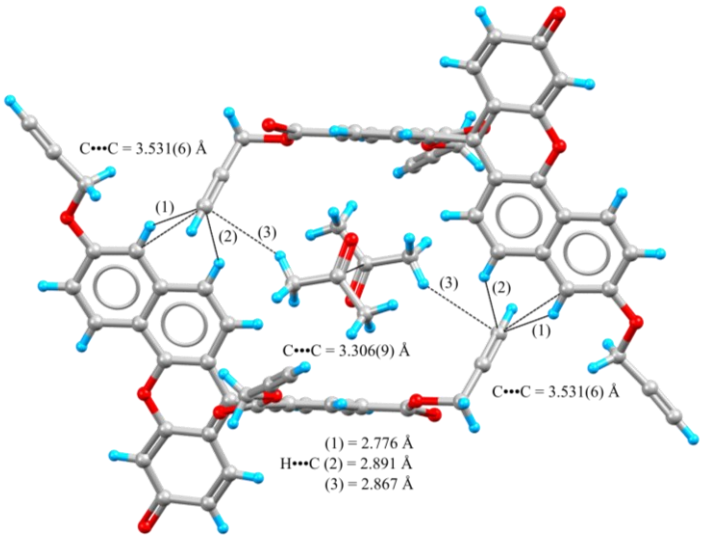

Figure S.71 *View of dimers on the phenyl group of TPRP-SNAFL showing interatomic distances. All short contacts between rendered molecules are depicted, using dashed lines. Atoms are rendered with a ball and stick depiction. Hydrogen positions are simulated as riding on their substituent, thus standard deviations are not determined for hydrogen bonds.*

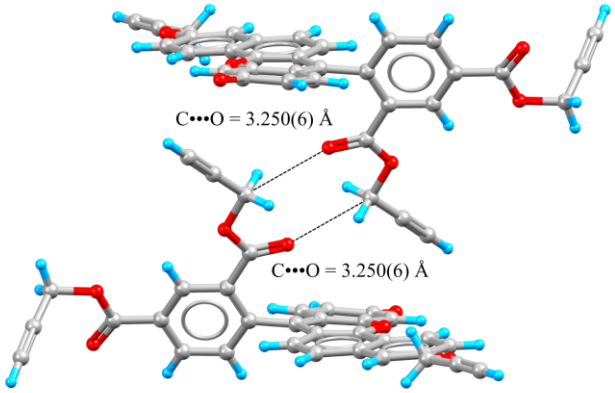

Figure S.72 *View of dimers on the phenyl group of TPRP-SNAFL showing interatomic distances. All short contacts between rendered molecules are depicted, using dashed lines. Atoms are rendered with a ball and stick depiction. Hydrogen positions are simulated as riding on their substituent, thus standard deviations are not determined for hydrogen bonds.*

4. Visualization of Aggregates

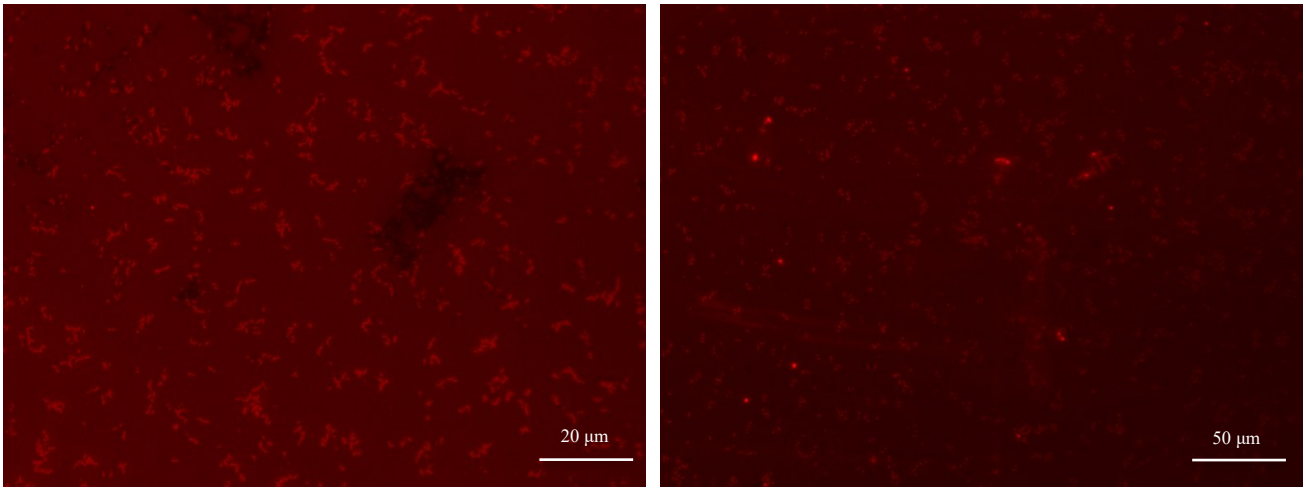

***Figure S**.73 Fluorescence microscopy images of DPRP-SNAFL (~1 µM in acetone with trace water) imaged at 40x and 63x (Cy3 filter)*

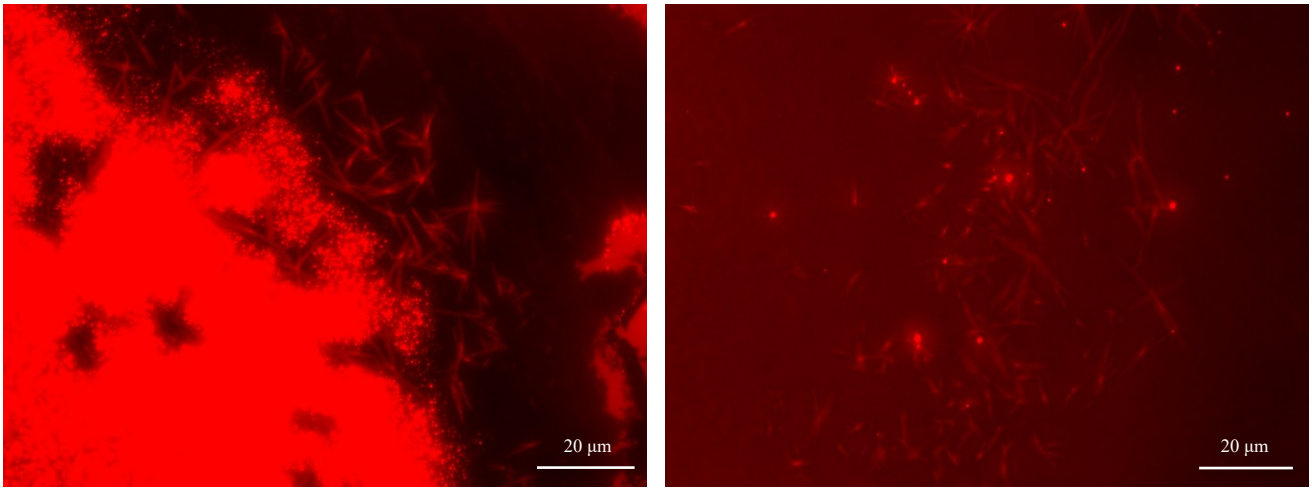

***Figure S**.74 Fluorescence microscopy images of DPRP-SNAFL (~1 µM in 70% water/acetone mixture) imaged at 63x (Cy3 filter) in proximity to the drying edge*

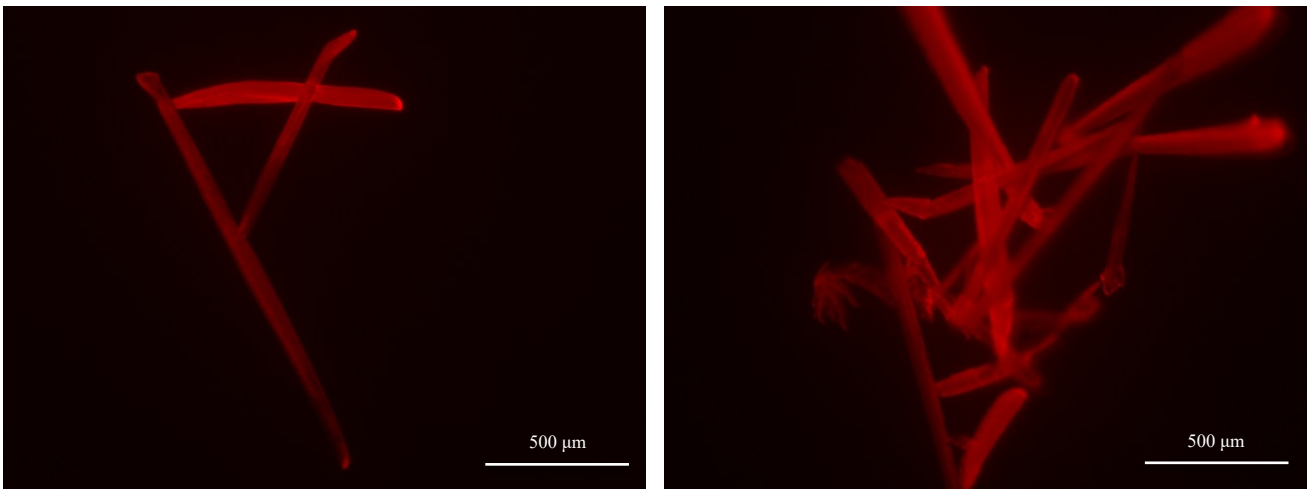

***Figure S**.75 Fluorescence microscopy images (Cy 3 filter) of aged TPRP-SNAFL (70% water/acetone mixture) solution*

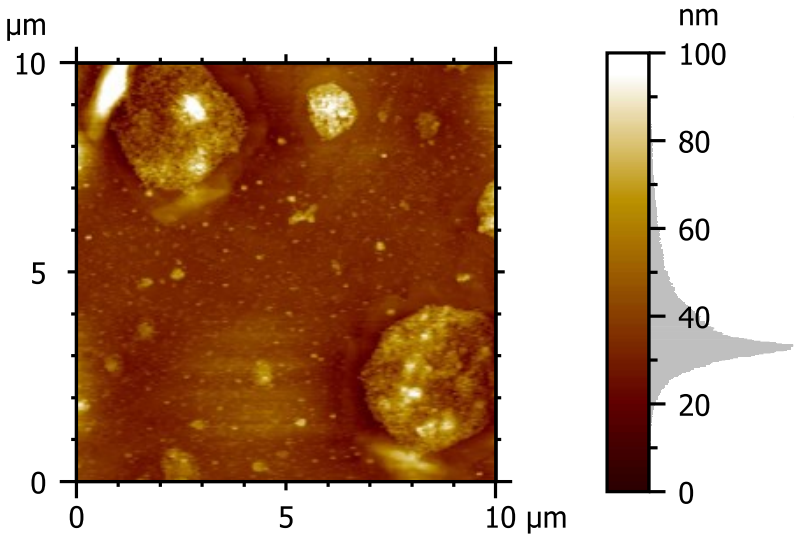

Figure S.76 *AFM image of DPRP-SNAFL aggregates (0.2 µM solution in 70% water/acetone, drop cast on silicon wafer)*

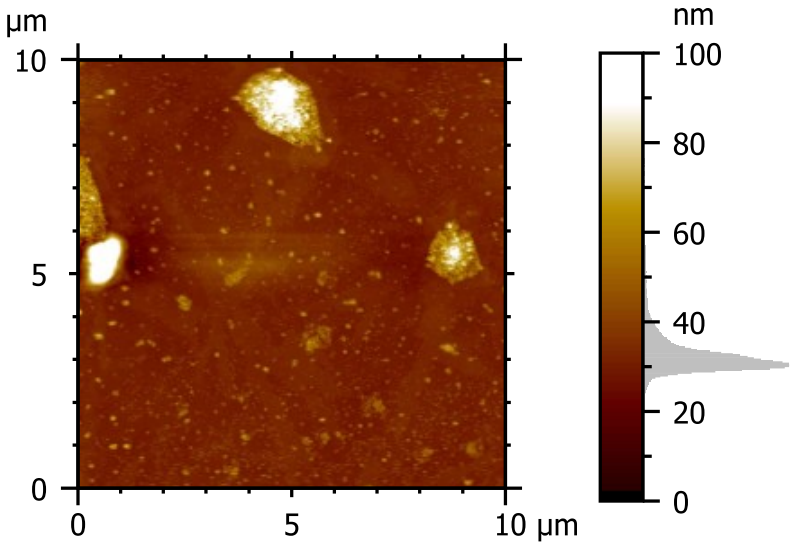

Figure S.77 *AFM image of DPRP-SNAFL aggregates (0.2 µM solution in 70% water/acetone, drop cast on silicon wafer)*

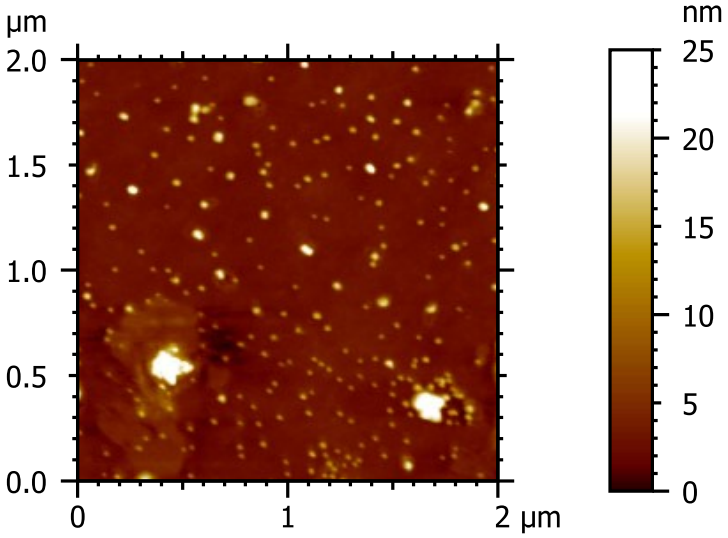

Method	Threshold detection		
Channel	HeightRetrace (1 / 4)		
Number of particles	226		
Coverage	3.843	%	
Density	56500000	Particles/mm²	
Individual results			
Parameters	Area	Mean diameter	Z-mean
Unit	µm²	µm	nm
Particle #1	0.001302	0.03876	13.54
Particle #2	0.0002626	0.01621	8.594
Particle #3	0.000797	0.02975	10.44
Particle #4	0.0003698	0.01971	8.389
Particle #5	0.0003095	0.01801	7.900
Particle #6	0.0004349	0.02172	8.921
Particle #7	0.0003375	0.01863	8.627
Particle #8	0.0003444	0.01885	7.995
Particle #9	0.001291	0.0387	12.51
Particle #10	0.001197	0.03688	9.692
Particle #11	0.0002774	0.01698	8.009
Particle #12	0.0008885	0.03164	10.28
Particle #13	0.00293	0.05856	12.27
Particle #14	0.0005838	0.02527	8.916
Particle #15	0.0004471	0.02184	8.627
Particle #16	0.001293	0.03896	11.65
Particle #17	0.0002025	0.01437	7.685
Particle #18	0.002776	0.05726	13.40
Particle #19	0.002084	0.04873	10.49
Particle #20	0.0003586	0.0195	8.447
Particle #21	0.0004754	0.02247	8.936
Global statistics			
Mean	0.0006829	0.02549	9.093

Figure S.78 *AFM image of DPRP-SNAFL aggregates (0.2 µM solution in 70% water/acetone, drop cast on silicon wafer) and particle size analysis, with elimination of large compound aggregates*

5. Biological Evaluation

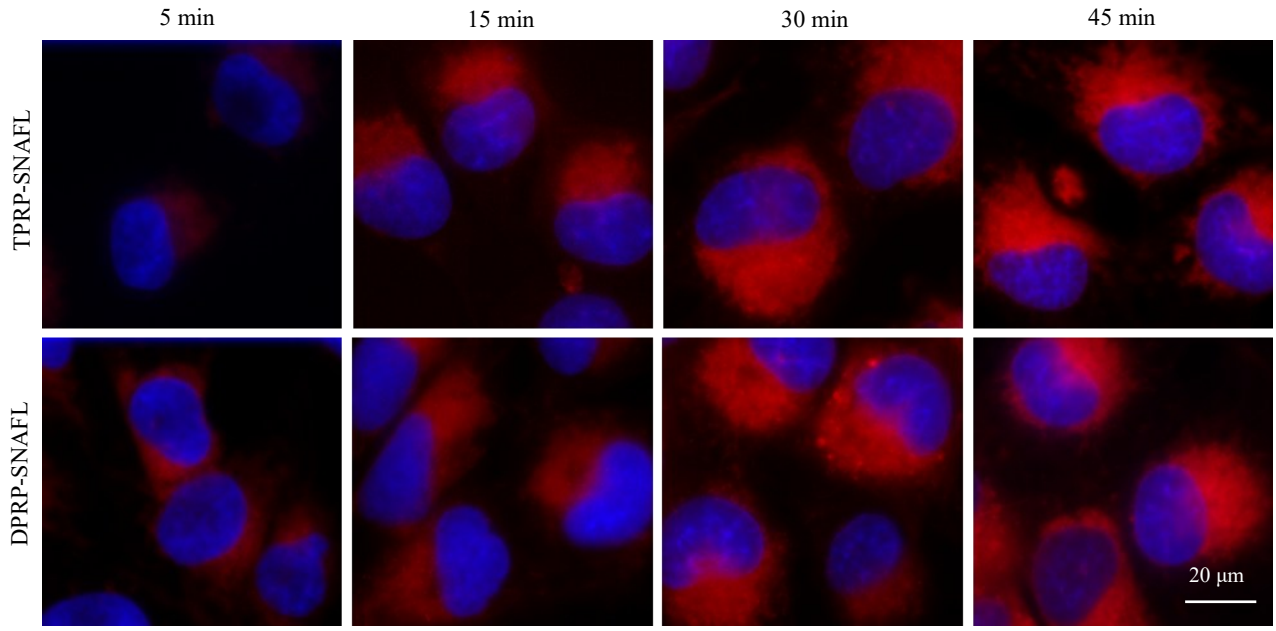

Figure S.79 *The intracellular fluorescence of TPRP-SNAFL and DPRP-SNAFL increases in a time dependent manner in human HMC3 microglia cells. Fluorescence micrographs of microglia cells treated with TPRP-SNAFL* ***1*** *or DPRP-SNAFL* ***2*** *(red, 1 µM) for 5, 15, 30 or 45 min in HBSS. Nuclei (blue) were labelled with Hoechst 33342. Cells were washed and imaged using a fluorescence microscope with the UV and Cy3 filters (DAPI-1160A, Semrock, ex: 387 nm, em: 447 nm; TRITC-A, Semrock, ex: 542 nm, em: 620 nm).*

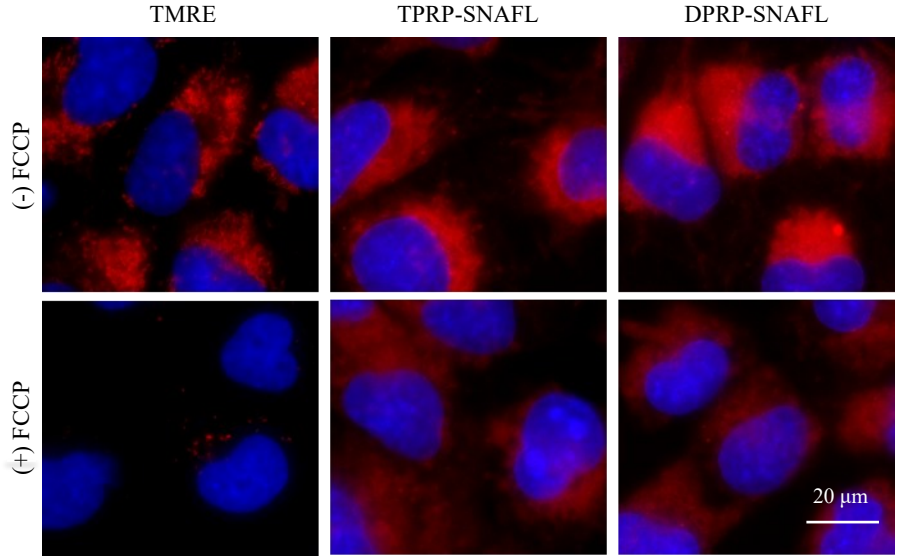

Figure S.80 *The intracellular fluorescence of TPRP-SNAFL and DPRP-SNAFL in response to decreased mitochondrial potential in human HMC3 microglia cells. Fluorescence micrographs of microglia cells treated with TMRE, TPRP or DPRP (red, 1 µM) with or without FCCP (20 µM) for 30 min in HBSS. Nuclei (blue) were labelled with Hoechst 33342. Cells were washed and imaged using a fluorescence microscope with the UV and Cy3 filters (DAPI-1160A, Semrock, ex: 387 nm, em: 447 nm; TRITC-A, Semrock, ex: 542 nm, em: 620 nm).*

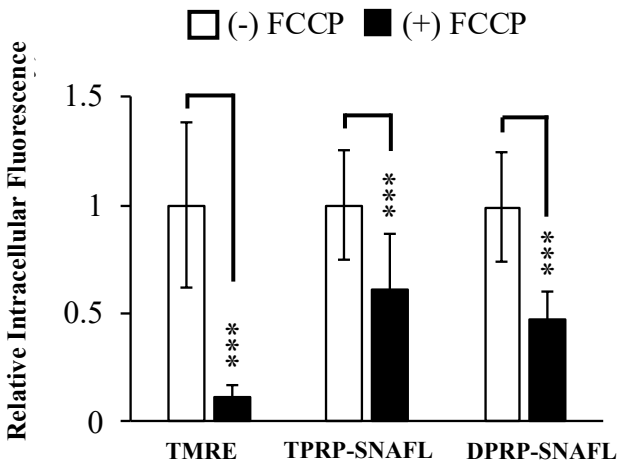

Figure S.81 *The intracellular fluorescence of TPRP-SNAFL and DPRP-SNAFL in response to decreased mitochondrial potential in human HMC3 microglia cells. Shown are the average level of intracellular fluorescence per cell, normalized to each control without FCCP (set to 1) ±SD from three independent experiments. At least 120 cells were analyzed per condition. Student's t-test with Bonferroni's correction. ***p<0.001.*

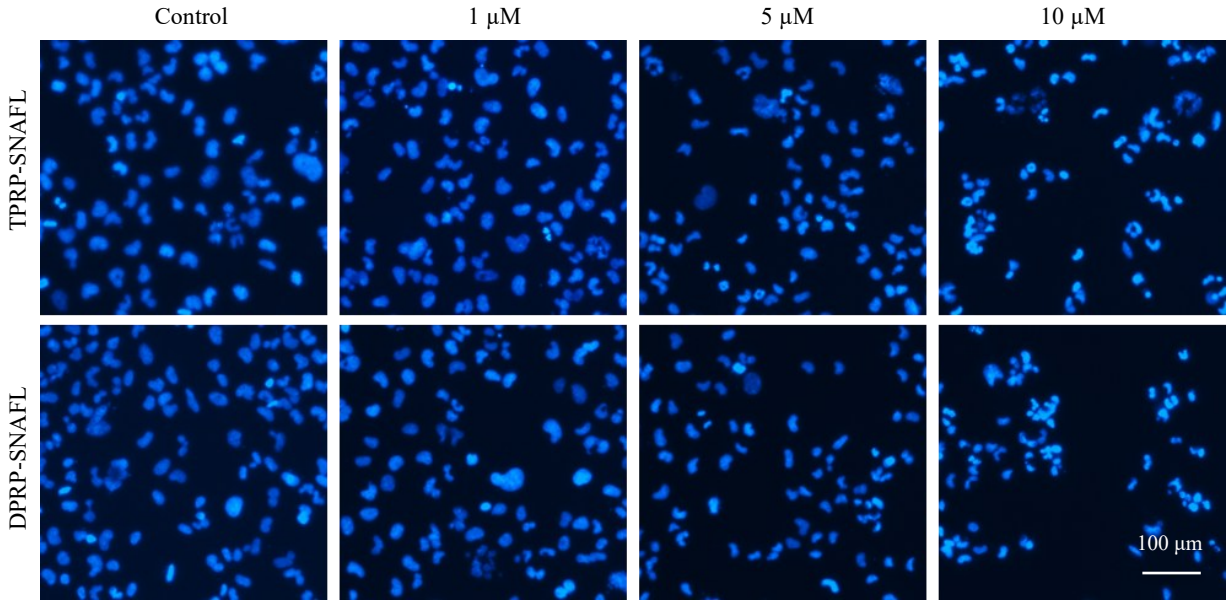

Figure S.82 *Fluorescence micrographs of microglia treated with increasing concentrations of TPRP or DPRP for 24 h. Nuclei (blue) were labelled with Hoechst 33342. Cells were imaged using a fluorescence microscope using the UV filter (DAPI-1160A, Semrock, ex: 387 nm, em: 447 nm).*

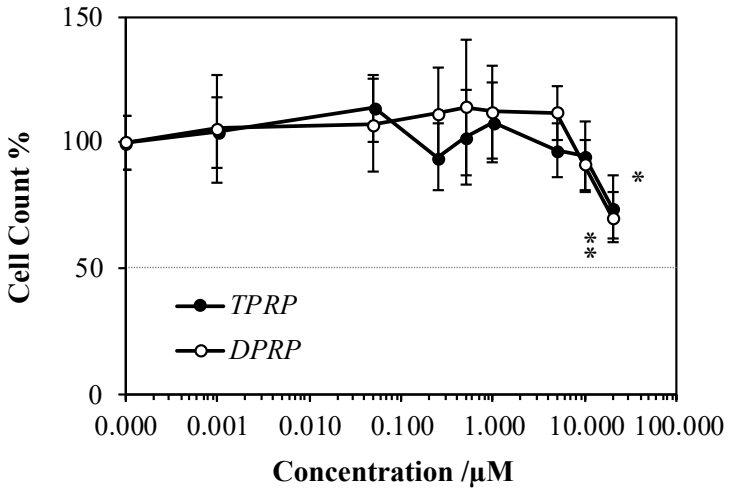

Figure S.83 *Dose-dependent cell viability in human HMC3 microglia cells*

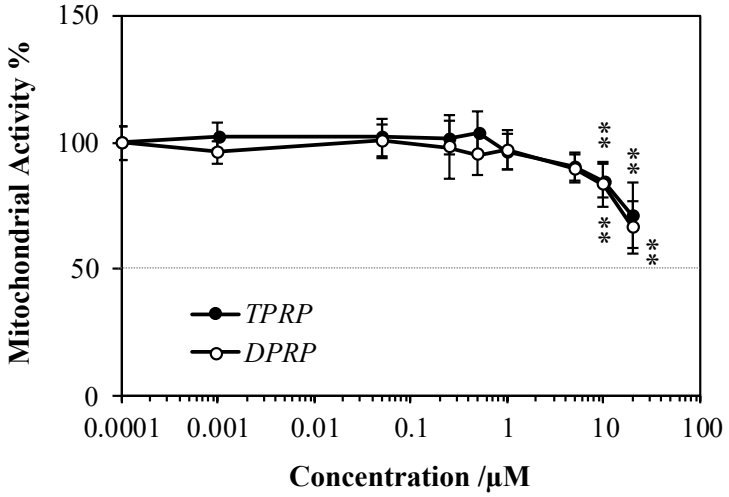

Figure S.84 *Dose-dependent mitochondrial metabolic activity in human HMC3 microglia cells. The average number of cells after treatment with TPRP-SNAFL or DPRP-SNAFL at concentrations 0.001, 0.05, 0.25, 0.5, 1, 5, 10, 20 µM. Shown are the percentage values relative to the untreated control (set to 100%) ±SD from three independent experiments. One-way ANOVA followed by Dunnett's test. *p<0.05, **p<0.01. (C) Mitochondrial metabolic activity in microglia treated for 24 h with* ***1*** *or* ***2*** *at 0.001, 0.05, 0.25, 0.5, 1, 5, 10, 20 µM was measured by the MTT assay. Shown are the average percentage of mitochondrial metabolic activity relative to the untreated control (100%) ±SD from three independent experiments. One-way ANOVA followed by Dunnett's test. **p<0.01*

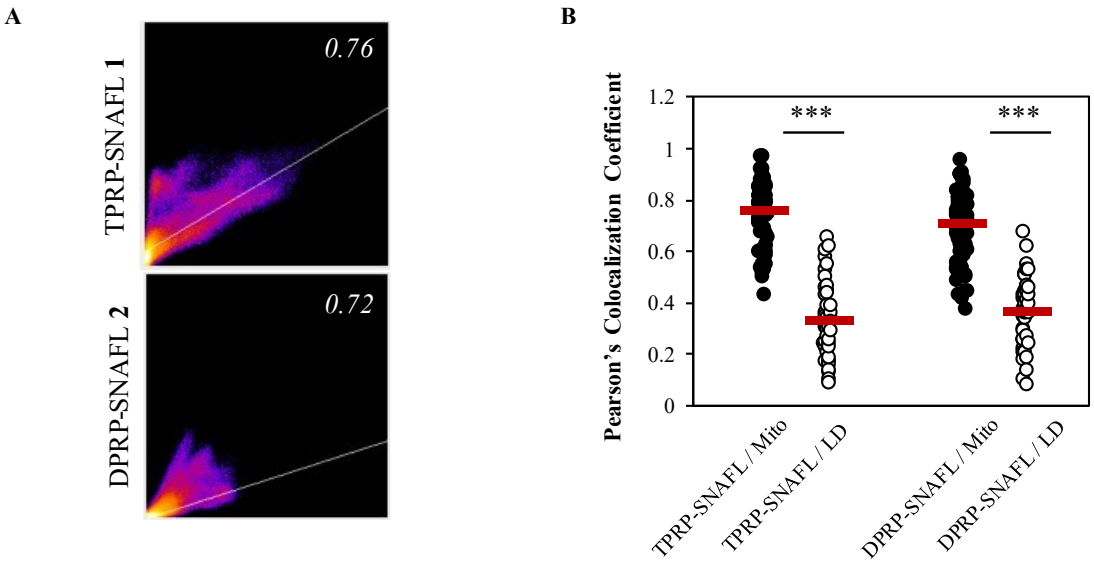

Figure S.85 *Pearson's colocalization coefficients for the fluorescence of TPRP-SNAFL (1 μM) and DPRP-SNAFL (1 μM) with mitochondria (Mito) and lipid droplets (LD). Mitochondria were fluorescently labelled with MitoTracker Deep Red, and lipid droplets were labelled with BODIPY 493/503. Human HMC3 microglia cells were imaged live using a fluorescence microscope after 30 min treatments. A) Shown are representative 2D intensity histograms for colocalization of TPRP-SNAFL and DPRP-SNAFL with mitochondria. B) Shown are the Pearson's colocalization coefficients per cell, from three independent experiments. The red bars indicate means from at least 47 cells. Student's t-test: ***p<0.001*

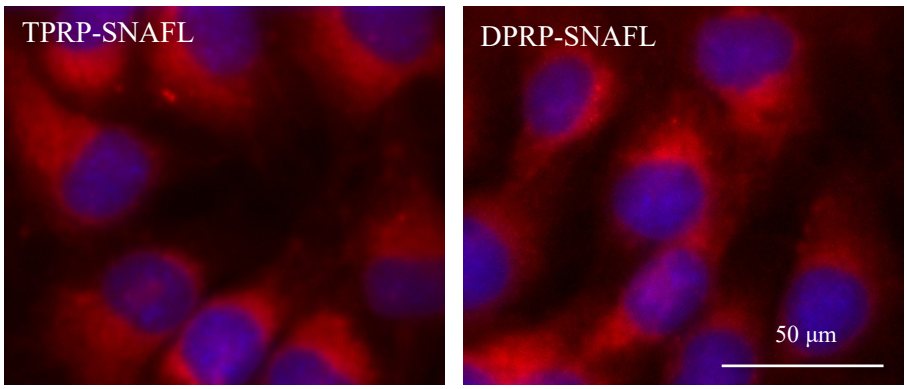

Figure S.86 *TPRP-SNAFL and DPRP-SNAFL retention in human HMC3 microglia cells after fixation with paraformaldehyde. Cells were treated with TPRP-SNAFL (1 μM) or DPRP-SNAFL (1 μM) for 30 min before fixation with paraformaldehyde (10 min). Cells were washed with phosphate-buffered salinand imaged using a fluorescence microscope (40X magnification) after 30 min. Luminogens (red) are retained in mitochondria, and nuclei (blue) were labelled with Hoechst 33342.*

References

1. L. McKay, N. Joma, D. Maysinger and A. Kakkar, *Journal of Materials Chemistry B*, 2025, **13**, 11790-11808.
2. A. Alessi, M. Salvalaggio and G. Ruzzon, *Journal of Luminescence*, 2013, **134**, 385-389.
3. S. S. Kurtz, Jr., A. E. Wikingsson, D. L. Camin and A. R. Thompson, *Journal of Chemical & Engineering Data*, 1965, **10**, 330-334.
4. K. Moutzouris, M. Papamichael, S. C. Betsis, I. Stavrakas, G. Hloupis and D. Triantis, *Applied Physics B*, 2014, **116**, 617-622.